Journal of Applied Analysis and Computation
Volume 13, Number 3, June 2023, 1388–1420
Website:http://www.jaac-online.com
DOI:10.11948/20220200

SOLITONS AND DOMAIN-WALL-ARRAY SOLUTIONS OF THE SCHRÖDINGER FLOW AND LANDAU-LIFSHITZ EQUATION

Penghong Zhong[1], Ye Chen[2,†], Song Chen[3] and Ganshan Yang[4]

Abstract We obtained some solitons and domain-wall-array solutions of the multidimensional Schrödinger flow and the Landau-Lifshitz equation using the homogeneous balance principle and general Jacobi elliptic-function method. These solutions include bright solitons and periodic solutions in terms of elliptic functions. We excluded several special types of solutions, such as kink profile solutions and dark solitons. The total phase profile of the solitons have two components: the kinematic origin, and the self-steepening effect. For the domain-wall-array solutions, the total phase profile consists of the kinematic origin, kinematic chirping, and self-steepening effect. In certain parameter domains, fundamental domain wall-array-solutions are chiral, and the propagation direction is determined by the sign of the self-steepening parameter. For ODEs deduced from Schrödinger flow that have no analytical solution, phase analysis is used to identify and classify the typical evolutionary pattern. Furthermore, the existence of limit cycles is verified, and the locations of singularities are precisely estimated.

Keywords Schrödinger flow, Landau-Lifshitz equation, soliton, domain wall.

MSC(2010) 35B07, 35B65.

1. Introduction

The nonlinear Schrödinger equation (NLSE) naturally arises in the mathematical modeling of various fields of physics, such as wave studies [16, 33, 34, 37], superconductivity (also known as Josephson effect across a Josephson junction) [24], quantum graph theory and its applications [4, 35], nonlinear optics [11, 15, 23], Bose-Einstein condensation (also know as the Gross Pitaevskii equation) [26, 30, 31] and even in mathematical finance [14, 40].

The NLSE has a general form

$$iu_t = \pm\triangle u + F(u,\, \bar{u},\, \nabla u,\, \nabla \bar{u}), \tag{1.1}$$

†The corresponding author.
Email: penghongzhong@yahoo.com(P. Zhong), yechent@nau.edu (Y. Chen), schen@uwlax.edu(S. Chen), yganshan@aliyun.com(G. Yang)
[1]Department of Applied Mathematics, Guangdong University of Education, Guangzhou 510640, China
[2]Department of Mathematics and Statistics, Northern Arizona University, Flagstaff, AZ 86011, USA
[3]Department of Mathematics and Statistics, University of Wisconsin - La Crosse, La Crosse, WI 54601, USA
[4]Department of mathematics, Yunnan Nationalities University, Kunming 650031, China

where $\triangle = \partial_{x_1}^2 + \cdots + \partial_{x_N}^2$, $\nabla u = (u_{x_1}, \ \dots \ , \ u_{x_N})$.

According to (1.1), the NLSE has the derivative and non-derivative type. One famous non-derivative case is the cubic Schrödinger equation arises in nonlinear optical systems. It is worth noting that some derivative cases have attracted more attention. For instance, the nonlinear Alfvén waves in space plasma [21]

$$iu_t = u_{x_1x_1} - \left(|u|^2 u\right)_{x_1},$$

and the sub-picosecond or femtosecond pulses in single mode optical fibers [22]

$$iu_t = \frac{1}{2}u_{x_1x_1} + R|u|^2 u - i\gamma\left(|u|^2 u\right)_{x_1},$$

where R and γ are the constant coefficients.

Both Alfvén waves model and femtosecond pulses model can be written as

$$iu_t = \pm\triangle u + F(u, \nabla u) \tag{1.2}$$

and this is the first order derivative equation.

Some efforts have been devoted to constructing the soliton of the derivative NLSE (1.2). In [6,13,38], the exact dynamic solutions which include several different solitons are discussed. As stated in [38], these solitons appear in quantum field theory, weakly nonlinear dispersive water waves and nonlinear optics when certain higher-order nonlinear effects are taken into account [6].

In this paper, we studied a famous derivative case with a special second order derivative, called Schrödinger flow (see [2,3,17,18]) as follows

$$iu_t = -\triangle u + \frac{2\bar{u}}{1+|u|^2}(\nabla u)^2. \tag{1.3}$$

This is a special case of the flow from one Riemannian manifold to a complex structure.

In another point of view, Schrödinger flow can be regarded as an equivalent equation of a spin vector equation called isotropic Landau-Lifshitz equation (ILLE).

$$S_t = S \times \triangle S, \tag{1.4}$$

where $S = (S_1, S_2, S_3)$ is on the ball $\mathbb{S}^2$ such that $S : \mathrm{R} \times \mathrm{R}^N \mapsto \mathbb{S}^2$ is a real valued map on $(t, x_1, \dots, x_N)$. Spin motions in diverse ferromagnetic structures are commonly described by the phenomenological Landau-Lifschitz equation (see, for example, [19]). The flow system (1.3) can be seen by applying the stereographic projection from $\mathbb{S}^2$ to C_∞, on the extended complex plane (the stereographic projection can be found in equation (6.5,6.6)). It describes the system in macroscopic language, in terms of the magnetization per unit volume S. In other words, in a classical limit based on a continuum model, Heisenberg model leads to the a simplest case of the Landau-Lifschitz equation – ILLE.

In the last three decades, a large amount of work has been devoted to the construction of exact solutions of nonlinear PDE. Various direct methods have been created to determine the exact solutions of NLSE, such as inverse scattering method [41], Darboux transformation [42], Hirota bilinear method [28], Jacobian elliptic function expansion method and the similarity transformation method [7].

For Ginzberg-Landau equation that is similar to NLSE, some powerful methods have been developed in finding the explicit solutions. These methods include inverse scattering transform, (G'/G)-expansion method, Hirota's bilinear method, exp-function expansion method, Jacobi elliptic function method, tanh-function method, extended trial function scheme, integration scheme etc. [5, 29, 39, 45].

Compare to non-derivative NLSE, little attention has been given to derivative NLSE. The exact solution of derivative case has not been widely studied compare to non-derivative case. In contrast to the NLSE without derivative ∇u, solving (1.3) (or (1.4)) is more opaque. In fact, the exact solutions of these two equations are rarely discussed in literature. Although the blowup property is confirmed in some work, such as [10, 20, 25], there is no exact explicit blowup solution of ILLE and Schrödinger flow presented in the literature. However, if the target $\mathbb{S}^2$ is replaced by the hyperbolic geometric manifold, the solution of the ILLE or Schrödinger flow can develop some finite time blowup [9]. We refer the readers to [44] for more detail of the exact finite time blowup and global solution. Till now, the exact explicit solutions for Schrödinger flow and ILLE are scarce as far as we know. For one dimensional case, the first general single-soliton solution is obtained by Tjon and Wright [36]. Similar to the work of Tjon and Wright, Azevedo et al. obtained a solitary-waves solution in [8]. Many years have passed after the work [8, 12, 36, 43], little or no result on the exact solution for ILLE or Schrödinger flow can be found. Hence, our goal in this paper is to obtain some wave solutions and to better understand the dynamic properties of these two equations.

It is well known that (1.2) admits some traveling wave solutions such as

$$u(t,\, x_1,\, \dots,\, x_N) = \mathrm{e}^{-i\omega\, t}\mathrm{e}^{if(\xi)}g\left(\xi\right), \tag{1.5}$$

where $\xi = \sum\limits_{j=1}^{N} k_j x_j - ct$. Hence, it is natural to ask whether the equation (1.3) has some solutions similar to (1.5), or equivalently, whether the equation (1.4) has some solutions similar to the following

$$S(t,\, x_1,\, \dots,\, x_N) = \left(\frac{2\cos(-\omega t + f\,(\xi))g(\xi)}{1+|g(\xi)|^2},\ \frac{2\sin(-\omega t + f\,(\xi))g(\xi)}{1+|g(\xi)|^2},\ \frac{1-|g(\xi)|^2}{1+|g(\xi)|^2}\right). \tag{1.6}$$

In this paper, we employed (1.5) to construct the explicit solution of the Schrödinger flow (1.3) (and (1.6) for the ILLE (1.4)). Based on the solutions we obtained, we studied the dynamical property of this system. It is well known that the main barrier to Schrödinger flow (or ILLE) is that there is no energy monotonicity inequality [10] for it. Hence, what solution will evolve after a long time is difficult to determine. However, the exact structure for the explicit solutions will help us to conquer this problem and to obtain the well-posedness result.

The paper is organized as follows. In section 2, the bell profile and singular profile solutions are constructed. In section 3, the exact solutions are obtained by using the general Jacobi elliptic-function method. In section 4, we studied the phase and singular point for the ordinary differential equation (ODE) derived from the Schrödinger flow. The graphs of some solutions and the phase diagram are provided in section 5. We compared our solutions of this paper with some other solutions in section 6.

2. Bell and singular profile solutions

If we set $u = v + iw$ and separate the real and imaginary part of (1.3), then

$$- w_t + \sum_{j=1}^{N} v_{x_j x_j} - \frac{2 \sum\limits_{j=1}^{N} v {v_{x_j}}^2}{(1+|u|)^2} + \frac{2 \sum\limits_{j=1}^{N} v {w_{x_j}}^2}{(1+|u|)^2} - \frac{4 \sum\limits_{j=1}^{N} w v_{x_j} w_{x_j}}{(1+|u|)^2} = 0, \tag{2.1}$$

and

$$v_t + \sum_{j=1}^{N} w_{x_j x_j} - \frac{4 \sum\limits_{j=1}^{N} v v_{x_j} w_{x_j}}{(1+|u|)^2} + \frac{2 \sum\limits_{j=1}^{N} w {v_{x_j}}^2}{(1+|u|)^2} - \frac{2 \sum\limits_{j=1}^{N} w {w_{x_j}}^2}{(1+|u|)^2}, \tag{2.2}$$

respectively.

We first looked for the plane wave solutions, both carrier and envelope waves in the following,

$$u = \mathrm{e}^{-i\omega\, t} \mathrm{e}^{i f(\xi)} g\left(\xi\right), \tag{2.3}$$

where ω is a real constant coefficient, $(k_1, k_2, ..., k_N)$ is a vector describing the direction of propagation, $f\left(\xi\right)$ and $g\left(\xi\right)$ are real function of ξ, and $\xi = \sum\limits_{j=1}^{N} k_j x_j - ct$ (k_j, c are the real constant coefficients) is the traveling variant with the inverse pulse width $(k_1, k_2, ..., k_N)$ and the inverse group velocity c.

We started with a new reduction for (2.1)-(2.2) by substituting (2.3) to (2.1) and (2.2), we obtained the real part and imaginary part equation in the following, respectively,

$$\begin{aligned} & k^2 g^3 (f')^2 + c g^3 f' + k^2 g^2 g'' - k^2 g (f')^2 - 2\, k^2 g (g')^2 \\ & + \omega g^3 + c g f' + k^2 g'' + \omega g = 0, \end{aligned} \tag{2.4}$$

and

$$k^2 g^3 f'' - 2\, k^2 g^2 f' g' - c g^2 g' + k^2 f'' g + 2\, k^2 f' g' - c g' = 0, \tag{2.5}$$

where $k^2 = \sum\limits_{j=1}^{N} k_j^2$.

It is difficult to determine the general solution of the nonlinear coupled ODEs (2.4)-(2.5). However, we can construct some special solutions for it. Solving (2.5), we have

$$f = \int \frac{\left(1 + g^2\right)\left(2\, C k^2 g^2 + 2\, C k^2 - c\right)}{2\; g^2 k^2}\, \mathrm{d}\xi, \tag{2.6}$$

where C can be an arbitrary complex constant. In this paper, we assume that C is a real constant. Let $2\, C k^2 - c = 0$. Then (2.6) can be simplified as

$$f = C \int \left(1 + g^2\right) \mathrm{d}\xi, \tag{2.7}$$

which can then be substituted into equation (2.4) to obtain a non-autonomous ODE in terms of g only

$$\mu_7 g^7 + \mu_5 g^5 + \mu_3 g^3 + \mu_1 g + g^2 g'' - 2\, g {g'}^2 + g'' = 0, \tag{2.8}$$

where

$$\mu_7 = 1, \qquad \mu_5 = \frac{k^2+2}{k^2},$$
$$\mu_3 = \frac{-C^2k^2 + 4\,C^2 + \omega}{C^2k^2}, \quad \mu_1 = \frac{-C^2k^2 + 2\,C^2 + \omega}{C^2k^2}.$$

We can reduce the number of parameters in (2.8) by assuming $C = 1$ and $k = 1$. Then (2.8) can be rewritten as

$$g^7 + 3\,g^5 + (3+\omega)\,g^3 + (1+\omega)\,g + g^2g'' - 2\,gg'^2 + g'' = 0. \tag{2.9}$$

Here we would like to point out that if $C = 0$, then $f = 0$ according to (2.7). If $C \neq 1$, then (2.8) will degenerate to an equation similar to (2.9) and so results similar solutions.

In order to solve (2.9), we introduced the auxiliary function

$$(g^{'})^2(\xi) = \sum_{j=0}^{6} h_j g^j(\xi), \tag{2.10}$$

where the coefficients h_js' are to be determined.

By (2.10), the second derivative g is

$$g^{''}(\xi) = \frac{1}{2}\sum_{j=1}^{6} j\,h_j g^{j-1}(\xi). \tag{2.11}$$

Substituting (2.10)-(2.11) to (2.9), we obtained an algebraic equation of g. If we set the coefficients of this polynomial equation to be 0, then

$$(g^{'})^2 = -g^6 + (C_1-2)g^4 + (\omega + 2C_1 - 1)g^2 + (\omega + C_1) = \sum_{j=0}^{6} h_j g^j(\xi). \tag{2.12}$$

According to Theorem 1 in [13], if $h_0 = h_1 = h_3 = h_5 = 0, h_6 < 0$, $h_4^2 - 4h_2h_6 > 0$, $h_2 > 0$ and $h_4 < 0$, then (2.12) has a bell profile solution

$$g(\xi) = \left\{\frac{2h_2\,\mathrm{sech}^2\sqrt{h_2}\,(\xi+\xi_0)}{2\sqrt{h_4^2 - 4h_2h_6} - \left(\sqrt{h_4^2-4h_2h_6} + h_4\right) sech^2\sqrt{h_2}\,(\xi+\xi_0)}\right\}^{\frac{1}{2}},$$

and a singular solution

$$g(\xi) = \left\{\frac{2h_2\,\mathrm{csch}^2\left[\pm\sqrt{h_2}\,(\xi+\xi_0)\right]}{2\sqrt{h_4^2-4h_2h_6} + \left(\sqrt{h_4^2-4h_2h_6} - h_4\right)\mathrm{csch}^2\left[\pm\sqrt{h_2}\,(\xi+\xi_0)\right]}\right\}^{\frac{1}{2}}.$$

If we let $C_1 = -\omega$, then $h_4^2 - 4h_2h_6 = \omega^2 > 0$. Furthermore, $-2 < \omega < -1$ leads to $h_2 > 0$ and $h_4 < 0$. So we have the following result.

Theorem 2.1. *If $-2 < \omega < -1$, then there exists some exact solutions of* (1.3) *as follows*

$$u = \mathrm{e}^{-i\omega\, t}\mathrm{e}^{i\int\left(1+g(\xi)^2\right)\,\mathrm{d}\xi}g\left(\xi\right), \tag{2.13}$$

where $\xi = \sum\limits_{j=1}^{N} k_j x_j - \frac{t}{2}$, $k^2 = \sum\limits_{j=1}^{N} k_j^2 = 1$,

$$g(\xi) = \left\{ \frac{-2(\omega+1)\,\mathrm{sech}^2\sqrt{-(\omega+1)}\,(\xi+\xi_0)}{2|\omega| - (|\omega|-\omega-2)\ \mathrm{sech}^2\sqrt{-(\omega+1)}\,(\xi+\xi_0)} \right\}^{\frac{1}{2}} \tag{2.14}$$

and

$$g(\xi) = \left\{ \frac{-2(\omega+1)\,\mathrm{csch}^2\left[\pm\sqrt{-(\omega+1)}\,(\xi+\xi_0)\right]}{2|\omega| + (|\omega|+\omega+2)\ \mathrm{csch}^2\left[\pm\sqrt{-\omega-1}\,(\xi+\xi_0)\right]} \right\}^{\frac{1}{2}}. \tag{2.15}$$

The corresponding exact solutions of (1.4) *are*

$$S = \left(\frac{2\cos(G(t,\xi))g(\xi)}{1+|g(\xi)|^2},\ \frac{2\sin(G(t,\xi))g(\xi)}{1+|g(\xi)|^2},\ \frac{1-|g(\xi)|^2}{1+|g(\xi)|^2} \right), \tag{2.16}$$

where

$$G(t,\xi) = -\omega t + \int\left(1+g\left(\xi\right)^2\right)\mathrm{d}\xi.$$

Remark 2.1. According to Theorem 2 of [13], if $h_1 = h_3 = h_5 = 0, h_0 = \frac{8{h_2}^2}{27h_4}$ and $h_6 = \frac{h_4^2}{4h_2}$ in (2.10), then there are two solutions.
(i) If $h_2 < 0$ and $h_4 > 0$, then (2.10) has a kink solution

$$g(\xi) = \left\{ -\frac{8h_2\tanh^2\left[\pm\sqrt{-\frac{h_2}{3}}\,(\xi+\xi_0)\right]}{3h_4\left(3+\tanh^2[\pm\sqrt{-\frac{h_2}{3}}\,(\xi+\xi_0)]\right)} \right\}^{\frac{1}{2}} \tag{2.17}$$

and a singular solution

$$g(\xi) = \left\{ -\frac{8h_2\coth^2\left[\pm\sqrt{-\frac{h_2}{3}}\,(\xi+\xi_0)\right]}{3h_4\left(3+\coth^2[\pm\sqrt{-\frac{h_2}{3}}\,(\xi+\xi_0)]\right)} \right\}^{\frac{1}{2}}. \tag{2.18}$$

(ii) If $h_2 > 0$ and $h_4 < 0$, then (2.10) has a triangular periodic solution

$$g(\xi) = \left\{ \frac{8h_2\tan^2\left[\pm\sqrt{\frac{h_2}{3}}\,(\xi+\xi_0)\right]}{3h_4\left(3-\tan^2\left[\pm\sqrt{\frac{h_2}{3}}\,(\xi+\xi_0)\right]\right)} \right\}^{\frac{1}{2}} \tag{2.19}$$

and a singular triangular periodic solution

$$g(\xi)=\left\{\frac{8h_2\cot^2\left[\pm\sqrt{\frac{h_2}{3}}\,(\xi+\xi_0)\right]}{3h_4\left(3-\cot^2\left[\pm\sqrt{\frac{h_2}{3}}\,(\xi+\xi_0)\right]\right)}\right\}^{\frac{1}{3}}. \tag{2.20}$$

However, by (2.12), a calculation indicates $h_0=\frac{8{h_2}^2}{27h_4}$, $h_6=\frac{h_4^2}{4h_2}$, $h_2<0$ and $h_4>0$ (or $h_2>0$ and $h_4<0$) do not hold at the same time. Hence the kink solution, singular solution, triangular periodic solution, and singular triangular periodic solution above do not exist.

We can also check that $h_0=h_1=h_3=h_5=0$, $h_6=\frac{k_4^2}{4h^2}$, $h_2>0$ and $h_4<0$ do not hold at the same time. According to the Theorem 3 of [13], we exclude the kink solution

$$g(\xi)=\left\{-\frac{h_2}{h_4}\left(1+\tanh\left[\pm\sqrt{h_2}(\xi+\xi_0)\right]\right)\right\}^{\frac{1}{2}} \tag{2.21}$$

and the singular solution

$$g(\xi)=\left\{-\frac{h_2}{h_4}(1+\coth[\sqrt{h_2}\,(\xi+\xi_0)])\right\}^{\frac{1}{2}}. \tag{2.22}$$

With some calculations, we can test that if (2.17 - 2.22) are substituted into the equation (2.10), then (2.10) holds if and only if the constraints $h_1=h_3=h_5=0$, $h_0=\frac{8{h_2}^2}{27h_4}$, $h_6=\frac{h_4^2}{4h_2}$ and $h_2h_4<0$ (or $h_0=h_1=h_3=h_5=0$, $h_6=\frac{k_4^2}{4h^2}$ and $h_2h_4<0$) are satisfied. This is why we excluded the solutions (2.17–2.22).

3. Jacobi elliptic function solutions

In this section, Jacobi elliptic function is applied in constructing solutions of (1.3). Similar to the steps in deriving Theorem 1, we use a 4-th order ODE (see (3.2)) to construct some other solutions. This method is used in [45] to construct the exact solutions of the Ginzberg-Landau equation. Substituting (2.6) to equation (2.4), we obtain an ODE

$$\left(k^2-\omega\right)g^3-\left(k^2+\omega\right)g+2\,{g'}^2g+g^2g''+g''=0. \tag{3.1}$$

We introduce the 4-th order auxiliary function

$$(g^{'})^2(\xi)=\sum_{j=0}^{4}q_jg^j(\xi) \tag{3.2}$$

and its second derivative

$$g^{''}(\xi)=\sum_{j=1}^{4}j\,q_jg^{(j-1)}(\xi), \tag{3.3}$$

where the coefficients q_j are to be determined.

Combining (3.2)-(3.3) with (3.1), we obtained a differential equation as follows

$$(g^{'})^2 = C_1 g^4 + \left(k^2 - \omega + 2\,C_1\right) g^2 - \omega + C_1 = \sum_{j=0}^{4} q_j g^j(\xi). \tag{3.4}$$

Similar to [45], with various $q_0,\ q_2,\ q_4$ in (3.4), we obtained the Jacobi elliptic function solutions in Table 1 as follows :

(i). If $q_0 = -(1-R^2)$, $q_2 = 2-R^2$, $q_4 = -1$ (just need to set $C_1 = -1$, $k = \pm\sqrt{-2R^2+4}$ and $\omega = -R^2$ in (2.12)), then it follows from Table 1 that $g(\xi) = \mathrm{dn}(\xi, R)$ where $\xi = \sum\limits_{j=1}^{N} k_j x_j - ct$ and $k^2 = \sum\limits_{j=1}^{N} k_j^2$. With $R \to 1$, $\mathrm{dn}(\xi, R) \to \mathrm{sech}(\xi)$.

(ii). If $q_0 = (1-R^2)$, $q_2 = 2R^2-1$ and $q_4 = -R^2$ (here we set $k^2 = 4\,R^2-2$, $\omega = -1$ and $C_1 = -R^2$ in (2.12)), then $g(\xi) = \mathrm{cn}(\xi, R)$ where $\xi = \sum\limits_{j=1}^{N} k_j x_j - ct$ and $k^2 = \sum\limits_{j=1}^{N} k_j^2$. With $R \to 1$, $\mathrm{cn}(\xi, R) \to \mathrm{sech}(\xi)$.

(iii). If $q_0 = -R^2$, $q_2 = 2R^2-1$ and $q_4 = 1-R^2$ (just set $k^2 = 4\,R^2-2$, $\omega = 1$ and $C_1 = -R^2+1$ in (2.12)), then $g(\xi) = \mathrm{nc}(\xi, R)$. With $R \to 1$, $\mathrm{nc}(\xi, R) \to \mathrm{ch}(\xi)$.

(iv). If $q_0 = -1$, $q_2 = 2-R^2$ and $q_4 = -1+R^2$ (just set $k^2 = -2\,R^2+4$, $\omega = R^2$ and $C_1 = R^2-1$ in (2.12)), then $g(\xi) = \mathrm{nd}(\xi, R)$. With $R \to 1$, $\mathrm{nd}(\xi, R) \to \mathrm{ch}(\xi)$.

The solutions (i)-(iv) are obtained according to Table 1. However, some solutions are missed. For example, if we suppose $q_4 = 0$, then

$$(g^{'})^2 = \left(k^2 - \omega\right) g^2 - \omega,$$

which includes the solutions

$$g\left(\xi\right) = \frac{\mathrm{e}^{K\xi}}{2\,\mathrm{e}^{C_2 K} K} + \frac{\mathrm{e}^{C_2 K}\omega}{2\,\mathrm{e}^{K\xi} K}$$

and

$$g\left(\xi\right) = \frac{\mathrm{e}^{C_2 K}}{2\,\mathrm{e}^{K\xi} K} + \frac{\mathrm{e}^{K\xi}\omega}{2\,\mathrm{e}^{C_2 K} K},$$

where $K = \sqrt{k^2 - \omega}$, C_2 is an arbitrary constant.

Based on the above discussion, we obtained the following result.

Theorem 3.1. *The exact solutions of* (1.3) *are as follows*

$$u = \mathrm{e}^{-i\omega\,t} \mathrm{e}^{i \int \frac{\left(1+g(\xi)^2\right)\left(2\,dk^2 g(\xi)^2 + 2\,dk^2 - c\right)}{2\,g(\xi)^2 k^2} \mathrm{d}\xi} g\left(\xi\right), \tag{3.5}$$

where c and d are constants, $\xi = \sum\limits_{j=1}^{N} k_j x_j - ct$ and $k^2 = \sum\limits_{j=1}^{N} k_j^2$.

The corresponding exact solutions of (1.4) *are*

$$\begin{pmatrix} S_1 \\ S_2 \\ S_3 \end{pmatrix} = \begin{pmatrix} \dfrac{2\cos\left(-\omega t + \displaystyle\int \frac{\left(1+g(\xi)^2\right)\left(2\,dk^2 g(\xi)^2 + 2\,dk^2 - c\right)}{2\,g(\xi)^2 k^2}\,\mathrm{d}\xi\right) g(\xi)}{1+|g(\xi)|^2} \\ \\ \dfrac{2\sin\left(-\omega t + \displaystyle\int \frac{\left(1+g(\xi)^2\right)\left(2\,dk^2 g(\xi)^2 + 2\,dk^2 - c\right)}{2\,g(\xi)^2 k^2}\,\mathrm{d}\xi\right) g(\xi)}{1+|g(\xi)|^2} \\ \\ \dfrac{1-|g(\xi)|^2}{1+|g(\xi)|^2} \end{pmatrix}. \tag{3.6}$$

We considered the following relations between k, R *and* w.

(i) If $k^2 = -2R^2 + 4$ *and* $\omega = -R^2$, *then*

$$g(\xi) = \mathrm{dn}(\xi, R). \tag{3.7}$$

With $R \to 1$, $\mathrm{dn}(\xi, R) \to \mathrm{sech}(\xi)$.

(ii) If $k^2 = 4\,R^2 - 2$ *and* $\omega = -1$, *then*

$$g(\xi) = \mathrm{cn}(\xi, R). \tag{3.8}$$

With $R \to 1$, $\mathrm{cn}(\xi, R) \to \mathrm{sech}(\xi)$.

(iii) If $k^2 = 4\,R^2 - 2$ *and* $\omega = 1$, *then*

$$g(\xi) = \mathrm{nc}(\xi, R). \tag{3.9}$$

With $R \to 1$, $\mathrm{nc}(\xi, R) \to \mathrm{ch}(\xi)$.

(iv) If $k^2 = -2\,R^2 + 4$ *and* $\omega = R^2$, *then*

$$g(\xi) = \mathrm{nd}(\xi, R). \tag{3.10}$$

With $R \to 1$, $\mathrm{nd}(\xi, R) \to \mathrm{ch}(\xi)$.

(v) If $K = \sqrt{k^2 - \omega} \neq 0$, *then*

$$g\,(\xi) = \frac{\mathrm{e}^{K\xi}}{2\,\mathrm{e}^{C_2 K} K} + \frac{\mathrm{e}^{C_2 K}\omega}{2\,\mathrm{e}^{K\xi} K}. \tag{3.11}$$

and

$$g\,(\xi) = \frac{\mathrm{e}^{C_2 K}}{2\,\mathrm{e}^{K\xi} K} + \frac{\mathrm{e}^{K\xi}\omega}{2\,\mathrm{e}^{C_2 K} K},$$

where C_2 *is an arbitrary constant.*

Remark 3.1. According to Table 1, we can exclude the solutions in the form of $\mathrm{ns}(\xi, R)$, $\mathrm{sc}(\xi, R)$, $\mathrm{sd}(\xi, R)$, $\mathrm{cs}(\xi, R)$, $\mathrm{cd}(\xi, R)$, $\mathrm{ds}(\xi, R)$ and $\mathrm{dc}(\xi, R)$ for (2.12) as the restriction on q_0 and q_2 and q_4 can not be satisfied at the same time.

Furthermore, (2.12) has some other special solutions in Jacobi elliptic function. Without lose generality, we assume $C_1 = \pm 1$. Then we can rewrite (2.12) as

$$(g^{'})^2 = \epsilon(g - A)(g - B)(g - C)(g - D), \tag{3.12}$$

Table 1. Solution of $(F^{'})^2(\xi) = \sum_{j=0}^{4} q_j F^j(\xi)$.

$F(\xi, R)$	q_0	q_2	q_4	$F(R \to 0)$	$F(R \to 1)$
ns	R^2	$-(1+R^2)$	1	csc	cth
dn	$-(1-R^2)$	$2-R^2$	-1	1	sech
cn	$1-R^2$	$2R^2-1$	$-R^2$	cos	sech
nc	$-R^2$	$2R^2-1$	$1-R^2$	sec	ch
nd	-1	$2-R^2$	$-(1-R^2)$	1	ch
sc	$1-R^2$	$2-R^2$	1	tg	sh
sd	$-R^2(1-R^2)$	$2R^2-1$	1	sin	sh
cs	1	$2-R^2$	$1-R^2$	ctg	ch
cd	R^2	$-(1+R^2)$	1	cos	1
ds	1	$2R^2-1$	$-R^2(1-R^2)$	csc	csch
dc	1	$-(1+R^2)$	R^2	sec	1

where A, B, C, D could have real or complex values.

Similar to [6], the solution of (3.12) has the following two cases.

(i) If $\epsilon = +1$, because A, B, C, D may not be all real, we can fix k and choose a large ω to get the real A and B as follows,

$$A = \frac{1}{2}\sqrt{-2\,k^2 + 2\,\omega - 4 + 2\sqrt{k^4 - 2\,k^2\omega + 4\,k^2 + \omega^2}} \quad \text{and} \quad B = -A. \tag{3.13}$$

At the same time, the complex C and D of (3.12) are

$$C = \frac{1}{2}\sqrt{-2\,k^2 + 2\,\omega - 4 - 2\sqrt{k^4 - 2\,k^2\omega + 4\,k^2 + \omega^2}} \quad \text{and} \quad D = -C. \tag{3.14}$$

respectively.

(ii) If $\epsilon = -1$, then $D < C < B < A$. Furthermore, if $-1 < \omega < 0$ and $k^2 > \omega + 2 + 2\sqrt{\omega + 1}$ (or $\omega > 0$ and $k^2 > \omega + 2 + 2\sqrt{\omega + 1}$), then

$$A = \frac{1}{2}\sqrt{2\,k^2 - 2\,\omega - 4 + 2\sqrt{k^4 - 2\,k^2\omega - 4\,k^2 + \omega^2}}, \quad D = -A. \tag{3.15}$$

$$B = \frac{1}{2}\sqrt{2\,k^2 - 2\,\omega - 4 - 2\sqrt{k^4 - 2\,k^2\omega - 4\,k^2 + \omega^2}} \quad \text{and} \quad C = -B. \tag{3.16}$$

Therefore, we obtain the following theorem.

Theorem 3.2. *In solution* (3.5) *and* (3.6)*, we have the following additional cases.*

(i) If $-1 < \omega < 0$, $k^2 > \omega + 2 + 2\sqrt{\omega + 1}$ (or $\omega > 0$ and $k^2 > \omega + 2 + 2\sqrt{\omega + 1}$), and A, B, C, D are defined in (3.15) *and* (3.16)*, then $g(\xi)$ can be the solutions (I) to (IV) in the Table 3.*

(ii) If $B < A < g(\xi)$, C and D are complex numbers with

$$(g^{'})^2 = (g - A)(g - B)(g - C)(g - D),$$

where A, B, C and D are defined in (3.13) *and* (3.14), *then*

$$g(\xi) = \frac{(A\beta - B\alpha) + (A\beta + B\alpha)\,\mathrm{cn}(\xi/G; K)}{(\beta - \alpha) + (\alpha + \beta)\,\mathrm{cn}(\xi/G; K)}$$

with $\alpha^2 = A^2 + (\mathrm{Im}C)^2$, $\beta^2 = B^2 + (\mathrm{Im}C)^2$, $G = (\alpha\beta)^{-1/2}$ *and* $K^2 = [(\alpha+\beta)^2 - (A-B)^2]/(4\alpha\beta)$.

Table 2. Solutions of $(F^{'})^2(\xi) = (F(\xi) - A)(F(\xi) - B)(F(\xi) - C)(F(\xi) - D)$.

	$F(\xi)$	Relationships
(I)	$\frac{D(A-C) - C(A-D)\,\mathrm{sn}^2(\xi/G;K)}{(A-C) - (A-D)\,\mathrm{sn}^2(\xi/G;K)}$, $G = \frac{2}{\sqrt{(A-C)(B-D)}}$, $K^2 = \frac{(A-D)(B-C)}{(A-C)(B-D)}$	$F(\xi) < D < C < B < A$
(II)	$\frac{C(B-D) - D(B-C)\,\mathrm{sn}^2(\xi/G;K)}{(B-D) - (B-C)\,\mathrm{sn}^2(\xi/G;K)}$, $G = \frac{2}{\sqrt{(A-C)(B-D)}}$, $K^2 = \frac{(A-D)(B-C)}{(A-C)(B-D)}$	$D < C < F(\xi) \leq B < A$
(III)	$\frac{B(A-C) - A(B-C)\,\mathrm{sn}^2(\xi/G;K)}{A-C) - (B-C)\,\mathrm{sn}^2(\xi/G;K)}$, $G = \frac{2}{\sqrt{(A-C)(B-D)}}$, $K^2 = \frac{(A-D)(B-C)}{(A-C)(B-D)}$	$D < C \leq F(\xi) < B < A$,
(IV)	$\frac{A(B-D) - B(A-D)\,\mathrm{sn}^2(\xi/G;K)}{(B-D) - (A-D)\,\mathrm{sn}^2(\xi/G;K)}$, $G = \frac{2}{\sqrt{(A-C)(B-D)}}$, $K^2 = \frac{(A-D)(B-C)}{(A-C)(B-D)}$	$D < C < B < A < F(\xi)$
(V)	$\frac{(A\beta - B\alpha) + (A\beta + B\alpha)\,\mathrm{cn}(\xi/G;K)}{(\beta-\alpha) + (\alpha+\beta)\,\mathrm{cn}(\xi/G;K)}$, $\alpha^2 = (A - \mathrm{Re}C)^2 + (\mathrm{Im}C)^2$, $\beta^2 = (B - \mathrm{Re}C)^2 + (\mathrm{Im}C)^2$, $G = (\alpha\beta)^{-1/2}$, $K^2 = \frac{(\alpha+\beta)^2 - (A-B)^2}{4\alpha\beta}$	$B < A < F(\xi)$

Remark 3.2. If $\epsilon = +1$, then $D < C < B < A$ does not hold for (3.12). Furthermore, if $B < A$, C and D are complex numbers, then $D = -\bar{C}$ does not hold at the same time. Hence, the solutions of the type (I) to (IV) do not exist according to Table 2.

Table 3. Solutions of $(F')^2(\xi) = -(F(\xi) - A)(F(\xi) - B)(F(\xi) - C)(F(\xi) - D)$.

	$F(\xi)$	Relationships
(I)	$\dfrac{D(A-C) + A(C-D)\,\mathrm{sn}^2(\xi/G;K)}{(A-C) + (C-D)\,\mathrm{sn}^2(\xi/G;K)}$, $G = \frac{2}{\sqrt{(A-C)(B-D)}}$, $K^2 = \frac{(A-B)(C-D)}{(A-C)(B-D)}$	$D < F(\xi) \le C < B < A$
(II)	$\dfrac{C(B-D) - B(C-D)\,\mathrm{sn}^2(\xi/G;K)}{(B-D) - (C-D)\,\mathrm{sn}^2(\xi/G;K)}$, $G = \frac{2}{\sqrt{(A-C)(B-D)}}$, $K^2 = \frac{(A-B)(C-D)}{(A-C)(B-D)}$	$D \le F(\xi) < C < B < A$
(III)	$\dfrac{B(A-C) - C(A-B)\,\mathrm{sn}^2(\xi/G;K)}{(A-C) - (A-B)\,\mathrm{sn}^2(\xi/G;K)}$, $G = \frac{2}{\sqrt{(A-C)(B-D)}}$, $K^2 = \frac{(A-B)(C-D)}{(A-C)(B-D)}$	$D < C < B < F(\xi) \le A$
(IV)	$\dfrac{A(B-D) + D(A-B)\,\mathrm{sn}^2(\xi/G;K)}{(B-D) + (A-B)\,\mathrm{sn}^2(\xi/G;K)}$, $G = \frac{2}{\sqrt{(A-C)(B-D)}}$, $K^2 = \frac{(A-B)(C-D)}{(A-C)(B-D)}$	$D < C < B \le F(\xi) < A$
(V)	$\dfrac{A\beta + B\alpha + (B\alpha - A\beta)\,\mathrm{cn}(\xi/G;K)}{\alpha + \beta + (\alpha - \beta)\,\mathrm{cn}(\xi/G;K)}$, $\alpha^2 = (A - \mathrm{Re}C)^2 + (\mathrm{Im}C)^2$, $\beta^2 = (\mathrm{B} - \mathrm{Re}C)^2 + (\mathrm{Im}C)^2$, $G = (\alpha\beta)^{-1/2}$, $K^2 = \frac{(A-B)^2 - (\alpha-\beta)^2}{4\alpha\beta}$	$B < A \quad C, D = -\bar{C}$

Remark 3.3. To compare the solutions obtained in the theorems (2.1)-(3.2) conveniently, they are summarized in Table 4.

4. Phase and singular point

In the previous two sections, we solved the ODEs with specific coefficients. There are many other cases that cannot be solved explicitly. In this section, we analyze the limit cycle and the singular points, and the direction field. Further analysis will be given in the next section.

Table 4. Three different types of solutions in Theorems (2.1)-(3.2).

Solutions I-III	$g\,(\xi)$
$u = \mathrm{e}^{-i\omega\, t}\mathrm{e}^{i\int \Theta_1\, \mathrm{d}\xi} g\,(\xi)\,,$ $\Theta_1 = 1 + g\,(\xi)^2,\ \xi = \sum_{j=1}^{N} k_j x_j - \frac{t}{2},$ $k^2 = \sum_{j=1}^{N} k_j^2 = 1$ and $-2 < \omega < -1$	$g(\xi) = \left\{ \frac{-2(\omega+1)\,\mathrm{sech}^2 \sqrt{-(\omega+1)}(\xi+\xi_0)}{2\lvert\omega\rvert - (\lvert\omega\rvert - \omega - 2)\,\mathrm{sech}^2 \sqrt{-(\omega+1)}(\xi+\xi_0)} \right\}^{\frac{1}{2}},$ $g(\xi) = \left\{ \frac{-2(\omega+1)\,\mathrm{csch}^2 \left[\pm\sqrt{-(\omega+1)}(\xi+\xi_0)\right]}{2\lvert\omega\rvert + (\lvert\omega\rvert + \omega + 2)\,\mathrm{csch}^2 \left[\pm\sqrt{-\omega-1}(\xi+\xi_0)\right]} \right\}^{\frac{1}{2}}$
$u = \mathrm{e}^{-i\omega\, t}\mathrm{e}^{i\int \Theta_2\, \mathrm{d}\xi} g\,(\xi),$ $\Theta_2 = \frac{\left(1+g(\xi)^2\right)\left(2\,dk^2 g(\xi)^2 + 2\,dk^2 - c\right)}{2\,g(\xi)^2 k^2},$ $\xi = \sum_{j=1}^{N} k_j x_j - ct$ and $k^2 = \sum_{j=1}^{N} k_j^2$	$g(\xi) = \mathrm{dn}(\xi, R),\ k^2 = -2R^2 + 4$ and $\omega = -R^2$ $g(\xi) = \mathrm{cn}(\xi, R),\ k^2 = 4\,R^2 - 2$ and $\omega = -1$ $g(\xi) = \mathrm{nc}(\xi, R),\ k^2 = 4\,R^2 - 2$ and $\omega = 1$ $g(\xi) = \mathrm{nd}(\xi, R),\ k^2 = -2\,R^2 + 4$ and $\omega = R^2$ $g\,(\xi) = \frac{\mathrm{e}^{K\xi}}{2\,\mathrm{e}^{C_2 K} K} + \frac{\mathrm{e}^{C_2 K}\omega}{2\,\mathrm{e}^{K\xi} K},\ K = \sqrt{k^2 - \omega} \neq 0$ $g\,(\xi) = \frac{\mathrm{e}^{C_2 K}}{2\,\mathrm{e}^{K\xi} K} + \frac{\mathrm{e}^{K\xi}\omega}{2\,\mathrm{e}^{C_2 K} K},\ K = \sqrt{k^2 - \omega} \neq 0$
$u = \mathrm{e}^{-i\omega\, t}\mathrm{e}^{i\int \Theta_2\, \mathrm{d}\xi} g\,(\xi),$ $\Theta_2 = \frac{\left(1+g(\xi)^2\right)\left(2\,dk^2 g(\xi)^2 + 2\,dk^2 - c\right)}{2\,g(\xi)^2 k^2},$ $\xi = \sum_{j=1}^{N} k_j x_j - ct$ and $k^2 = \sum_{j=1}^{N} k_j^2$	$g(\xi) = \frac{D(A-C) + A(C-D)\,\mathrm{sn}^2(\xi/G;K)}{(A-C) + (C-D)\,\mathrm{sn}^2(\xi/G;K)},$ $D < g(\xi) \le C < B < A$ $g(\xi) = \frac{C(B-D) - B(C-D)\,\mathrm{sn}^2(\xi/G;K)}{(B-D) - (C-D)\,\mathrm{sn}^2(\xi/G;K)},$ $D \le g(\xi) < C < B < A$ $g(\xi) = \frac{B(A-C) - C(A-B)\,\mathrm{sn}^2(\xi/G;K)}{(A-C) - (A-B)\,\mathrm{sn}^2(\xi/G;K)},$ $D < C < B < g(\xi) \le A$ $g(\xi) = \frac{A(B-D) + D(A-B)\,\mathrm{sn}^2(\xi/G;K)}{(B-D) + (A-B)\,\mathrm{sn}^2(\xi/G;K)},$ $D < C < B \le g(\xi) < A$ $g(\xi) = \frac{(A\beta - B\alpha) + (A\beta + B\alpha)\,\mathrm{cn}(\xi/G;K)}{(\beta-\alpha) + (\alpha+\beta)\,\mathrm{cn}(\xi/G;K)},$ $B < A < g(\xi)$

In (2.8), let $C = 1$. Then

$$g^7 + \lambda_5 g^5 + \lambda_3 g^3 + \lambda_1 g + g^2 g'' - 2\,g g'^2 + g'' = 0, \tag{4.1}$$

where

$$\lambda_1 = \frac{-k^2 + 2\, + \omega}{k^2}, \quad \lambda_3 = \frac{-k^2 + 4 + \omega}{k^2}, \quad \lambda_5 = \frac{k^2 + 2}{k^2}.$$

And let $g(\xi) = y(\xi)$. Then (4.1) can be converted to a system of first order differential equations

$$\begin{cases} y' = z \triangleq X_1(y,\, z), \\ z' = -\dfrac{y^7 + \lambda_5 y^5 + \lambda_3 y^3 - 2\,z^2 y + \lambda_1 y}{y^2+1} \triangleq Y_1(y,\, z), \end{cases} \tag{4.2}$$

where $\triangleq$ means 'is defined to be'.

Theorem 4.1. *If $\mathbf{D}_i^*$ is any connected sub-domain of $\mathbf{D}_i$ in the quadrant i ($i = 1,2,3,4$), then the system* (4.2) *satisfies the following properties.*

(i) There is no periodic solution and limit cycle in $\mathbf{D}_i^*$.

(ii) If the limit cycle of (4.2) *exists in yz-plan, then it oscillates around y axis.*

Proof. We prove by way of contradiction. Assume that there exists a periodic solution in the i-th quadrant $\mathbf{D}_i$ with period T, and the closed curve

$$\Gamma_i : y = y(\xi), \quad z = z(\xi), \quad 0 \leqslant \xi \leqslant T,$$

has the closed region $\mathbf{D}_{\Gamma_i}$ contained in $\mathbf{D}_i$, and Γ_i is the boundary of $\mathbf{D}_{\Gamma_i}$.

By Green's function, we have

$$\begin{aligned} &\iint_{\mathbf{D}_{\Gamma_i}} \left(\frac{\partial X_1}{\partial y} + \frac{\partial Y_1}{\partial z}\right) \mathrm{d}y\mathrm{d}z = \int_{\Gamma_i} (X_1 \mathrm{d}z - Y_1 \mathrm{d}y) \\ &= \int_0^T \left(X_1 \frac{\mathrm{d}z}{\mathrm{d}\xi} - Y_1 \frac{\mathrm{d}y}{\mathrm{d}\xi}\right) \mathrm{d}\xi = \int_0^T (X_1 Y_1 - Y_1 X_1) \mathrm{d}\xi = 0. \end{aligned} \tag{4.3}$$

As

$$\frac{\partial X_1}{\partial y} + \frac{\partial Y_1}{\partial z} = \frac{4\,zy}{y^2+1}$$

we then have that

$$\iint_{\Gamma_i} \left(\frac{\partial X_1}{\partial y} + \frac{\partial Y_1}{\partial z}\right) \mathrm{d}y\mathrm{d}z \neq 0, \tag{4.4}$$

and so (4.3) contradicts to (4.4). Therefore, There is no periodic solution and limit cycle in $\mathbf{D}_i$.

If the limit cycle of (4.2) exists in yz-plan, then it oscillates around a singular point on y axis. □

Similarly, in (3.1), we let $g(\xi) = y(\xi)$. Then it can be converted to a system of first order differential equations

$$\begin{cases} y' = z \triangleq X_2(y,\, z), \\ z' = -\dfrac{\left(k^2 - \omega\right) y^3 - \left(k^2 + \omega\right) y + 2\,z^2 y}{y^2+1} \triangleq Y_2(y,\, z). \end{cases} \tag{4.5}$$

Similar to Theorem (4.1), we have the following result.

Theorem 4.2. *If $\mathbf{D}_i^*$ is any connected sub-domain of $\mathbf{D}_i$ in the quadrant i ($i = 1,2,3,4$), then the system* (4.5) *satisfies the following properties.*

(i) There is no periodic solution and limit cycle in $\mathbf{D}_i^*$.

(ii) If the limit cycle of (4.5) *exists in yz-plan, then it oscillates around y axis.*

The equation (4.2) and (4.5) can not be converted to a Hamiltonian system on y and z as the function on the right hand side of (4.5) has a non-linear term z^2y, i.e., the function $H_j(y,z)$ $(j=1,2)$ does not exist such that

$$\begin{cases} \dfrac{\partial}{\partial y} H_j\,(y,z) = X_j, \\ \dfrac{\partial}{\partial z} H_j\,(y,z) = Y_j. \end{cases}$$

So (4.2) and (4.5) have no Hamiltonian function $H_j(y,z)$.
By (4.2), the singular points could be

$$(0,\,0), \quad or \quad (\pm\sqrt{\frac{-1+\sqrt{k^4-k^2\omega-2\,k^2+1}}{k^2}},\,0).$$

Similarly, the singular points of (4.5) are as follows

$$(0,\,0), \quad (\pm\sqrt{\frac{k^2+\omega}{k^2-\omega}},\,0).$$

As a summary, the center of the limit cycle of Theorem 4.1 and 4.2 is overlap with the above singular points. In the next section, we are to combine the phase diagram of (4.2),(4.5) and discuss the solution. We will also categorize the singular points and study how they transform to each other.

5. Geometric properties of the Solutions

In this section, we are to discuss the phase and singularity described in section 4 and characterize the geometry properties of the solutions obtained in sections 2 and 3.

5.1. Direction field of the (4.2) and (4.5)

We can see that the singular points presented in Figure 1 - 4 are centers and saddle points. We substituted specific values of k, w to see how the direction field of (4.2) changes, and the discussion is in the following. (i) If $\omega = k^2-2$, then $-1+\sqrt{k^4-k^2\omega-2\,k^2+1} = 0$, and the singular point of (4.2) is therefore (0, 0). We let $k=-1$ and $\omega=-1$, then the singular point of (4.2) is (0, 0). To observe the change of the singular point, we fix $\omega=-1$ and shift k such that $-1+\sqrt{k^4-k^2\omega-2\,k^2+1} \neq 0$. Here, k is selected from the values $\{-1,-9/8,-3/2,-10\}$. As we can see in the Figure 1, only the subplot (a) has one singular point which is also a central singularity, and (b,c,d) have three singular points where one in the origin and the other two are on the y-axis. With k decreasing from -1 to -10, the distance between the two singular points is increasing, we can also verify this by computing the corresponding y-coordinates of singular points from $\sqrt{(-1+\sqrt{k^4-k^2\omega-2k^2+1})/k^2}$, which gives us $\{0, 0.35, 0.65, 1.01\}$.

(ii) If $k=\sqrt{3}$ and $\omega=1$, then the singular point of (4.2) is (0, 0). Similar to (i), we fix $\omega=1$, and select k from $\{\sqrt{3},\ \sqrt{3}+1/8,\ \sqrt{3}+1/2,\ \sqrt{3}+9\}$, (4.2). By Figure 2, all the singular points are on the y-axis. With k increasing from $\sqrt{3}$ to

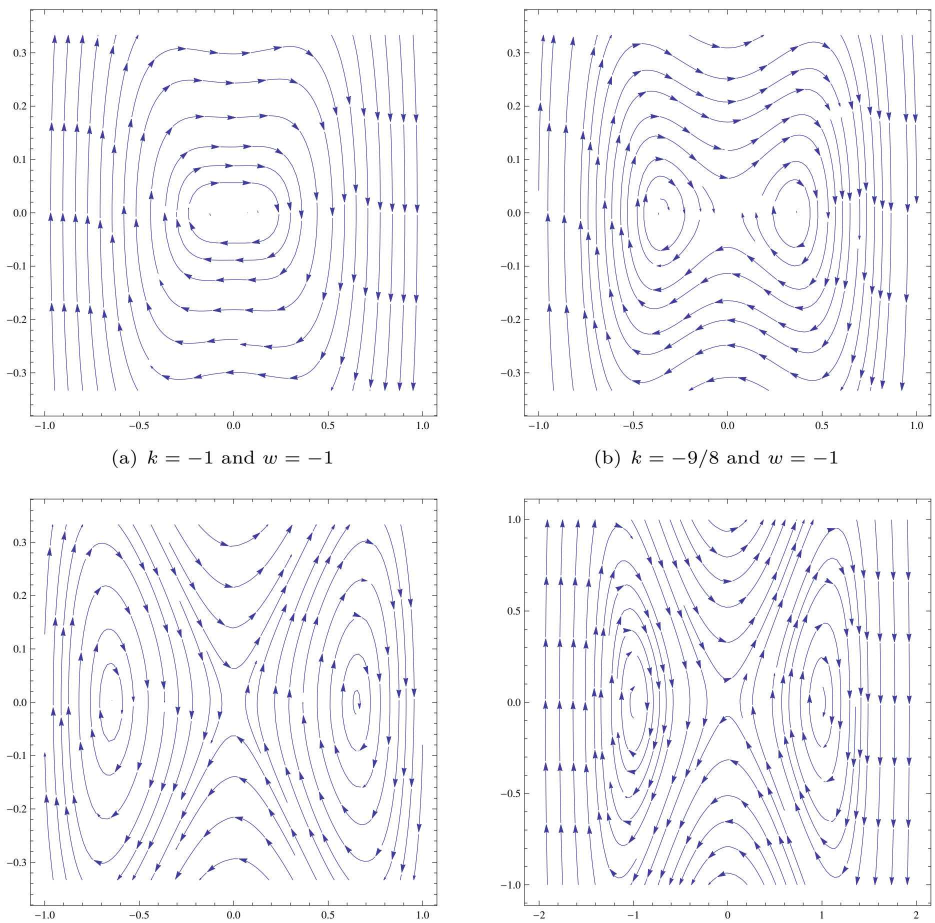

(a) $k = -1$ and $w = -1$

(b) $k = -9/8$ and $w = -1$

(c) $k = -3/2$ and $w = -1$

(d) $k = -10$ and $w = -1$

Figure 1. The direction field of (4.2) with different values of k and the same w.

$\sqrt{3} + 9$, the distance between the two singular points is increasing. We can also verify this by computing the corresponding y-coordinates of singular points from $\sqrt{(-1 + \sqrt{k^4 - k^2\omega - 2k^2 + 1})/k^2}$, which gives us $\{0, 0.42, 0.68, 0.99\}$. Moreover, with k increasing from $\sqrt{3}$ to $\sqrt{3} + 1/8$, the only central singularity in the subplot (a) splits into two central singularities on the y-axis, and leaving the origin as a saddle points in (b). With k increasing from $\sqrt{3} + 1/8$ to $\sqrt{3} + 9$, the central saddle point in (b) becomes a central singularity in (c,d), and the two central singularities in (b) on the y-axis became saddle points in (c,d).

(iii) We now look at the singular points of (4.5) in the following,

$$(0,\, 0), \quad (\pm\sqrt{\frac{k^2 + \omega}{k^2 - \omega}},\, 0).$$

With $k = 1$, $w = -1$, the equation (4.5) has only one singular point in the origin. We fix $\omega = -1$, and select k from $\{1, 9/8, 3/2, 10\}$. As we can see in Figure 3, when k is increasing from 1 to 10, the central singularity in (a) splits into two central

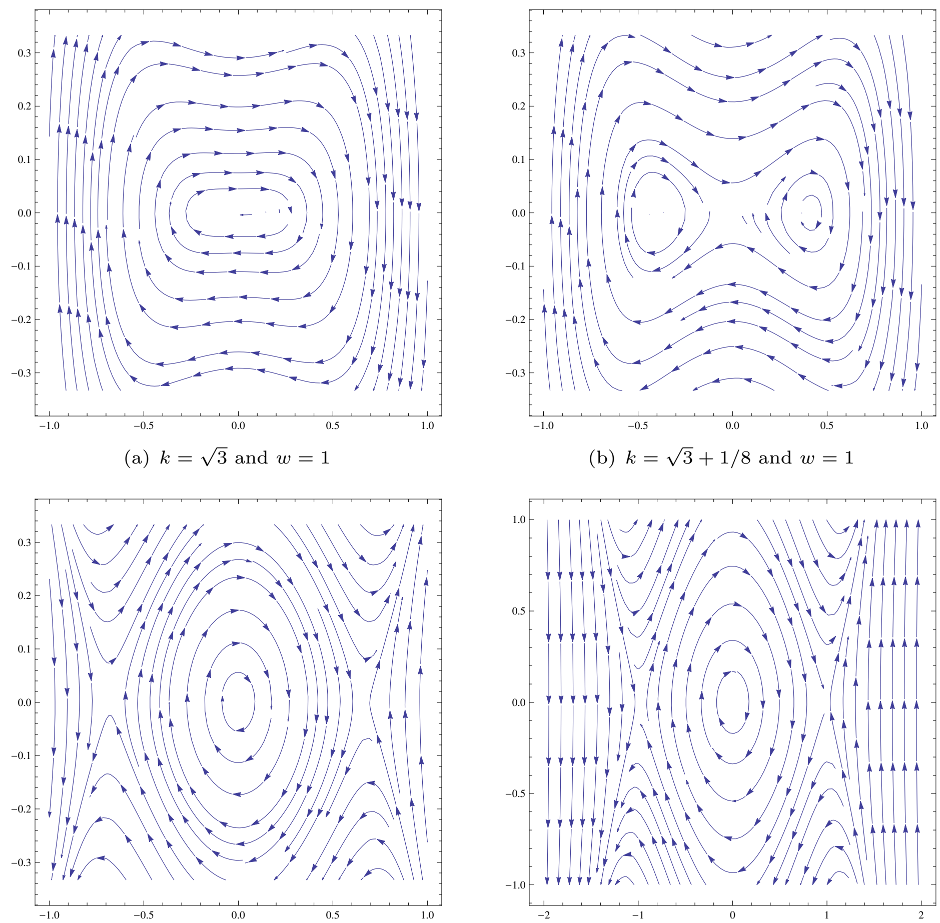

(a) $k = \sqrt{3}$ and $w = 1$

(b) $k = \sqrt{3} + 1/8$ and $w = 1$

(c) $k = \sqrt{3} + 1/2$ and $w = 1$

(d) $k = \sqrt{3} + 9$ and $w = 1$

Figure 2. The direction field of (4.2) with different values of k and the same w.

singularities on the y-axis in (b,c,d), and leaving the origin as a saddle point in (b,c,d). Moreover, the solutions become more vertical from (a) to (d).

(iv) In Figure 4, we fix $\omega = 1$, and select k from $\{1, 9/8, 3/2, 10\}$. As $w = 1$, the denominator $k^2 - \omega$ can be 0, and therefore, there are horizontal solutions in (a). When k is increasing from 1 to 10, the central singularity stays the same as a saddle point. Similar to the Figure 3, the solution curves are more vertical from (a) to (d).

5.2. Bright soliton and Jacobi elliptic function solution

The figures of two different kinds of solution which include bright soliton and Jacobi elliptic function solution are presented in this section. Based on these figures, the properties of these solutions are summarized in the following.

(i) We can see the evolution of $|u|$ for the bright solution (2.13)-(2.14) in Figure 5 (a). The evolution of u for the solution (2.13)-(2.15) is similar to Figure 5 (a).

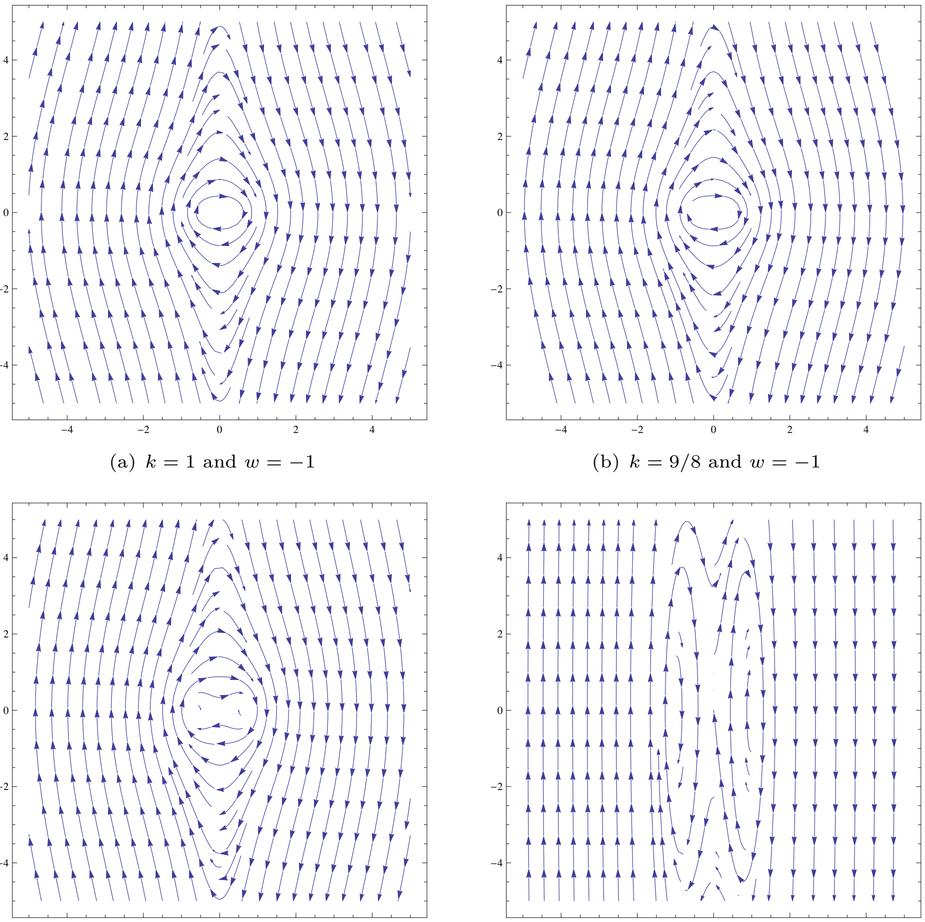

(a) $k = 1$ and $w = -1$

(b) $k = 9/8$ and $w = -1$

(c) $k = 3/2$ and $w = -1$

(d) $k = 10$ and $w = -1$

Figure 3. The direction field of (4.5) with different values of k and the same w.

The value of ω determines the magnitude of the domain wall array. The value of ξ_0 determines the center of the peak, and different ξ_0 does not change the shape of the solution. (ii) The phase profile of Figure 5 (a) is ploted in Figure 5 (b). The phase derivative changes simultaneously with the bright soliton, and it is computed by $1 + |u|^2$ for the solution (2.13)-(2.14). The constant 1 is the kinematic origin, the second term $|u|^2$ comes from the self-steepening effect. From the Figure 5 (b), the phase is similar to the module $|u|$, i.e., the phase is similar to its solution (2.13)-(2.14).

(iii) For the solution (3.5) in Figure 6 (a), with R approaching 1 from the left, the amplitude and the intensity of the solution are increasing.

Each curve in Figure 6 (b) can be decomposed into three sections. In fact, the phase $2 - 1/2\, k^{-2} + g^{-2} - 1/2\, k^{-2} g^{-2} + g^2$ can be split into three parts: the term $2 - 1/2\, k^{-2}$ is of kinematic origin, the term $g^{-2} - 1/2\, k^{-2} g^{-2}$ leads to the kinematic chirping (see Figure 6 (a)), and the term g^2 comes from the self-steepening effect (see Figure 6 (b)). The contribution of the higher-order chirping (Figure 7(b))

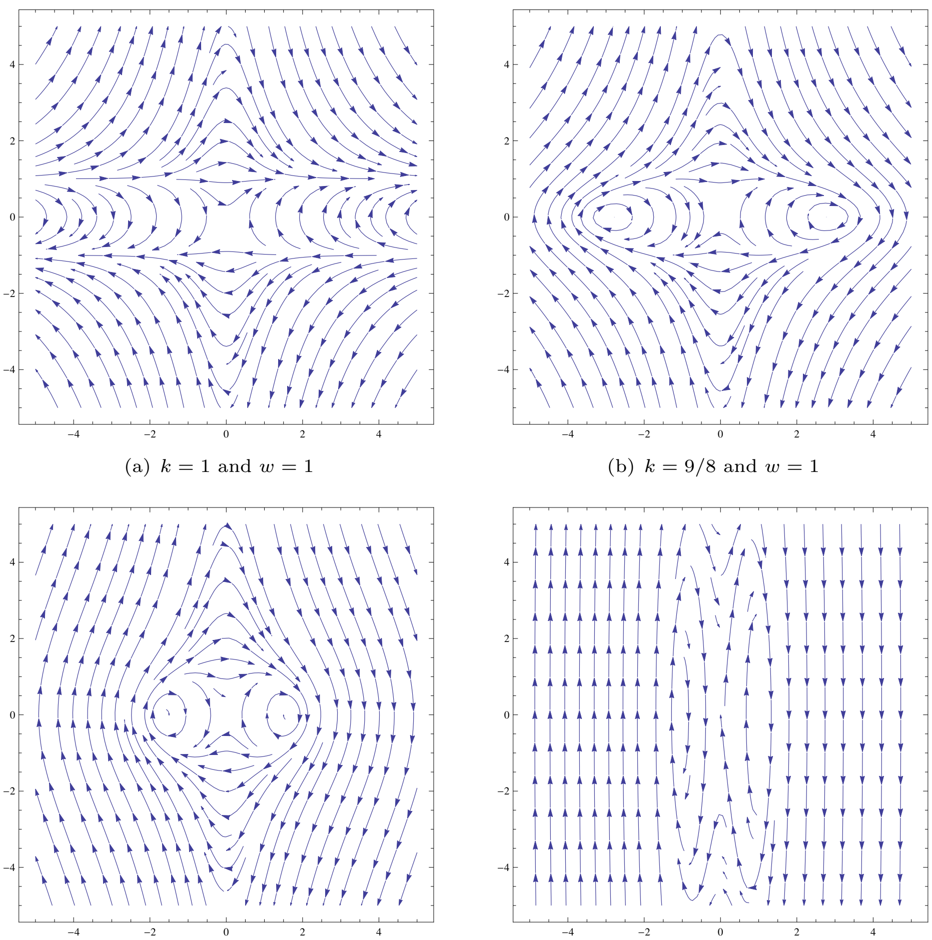

(a) $k = 1$ and $w = 1$

(b) $k = 9/8$ and $w = 1$

(c) $k = 3/2$ and $w = 1$

(d) $k = 10$ and $w = 1$

Figure 4. The direction field of (4.5) with different values of k and the same w.

partially offset that of the kinematic chirping (Figure 7(a)), and thus the range of the total phase is smaller than that of the kinematic chirping. (iv) Figure 8 (a) and (b) are contour curves of the real part of the bright soliton (2.13)-(2.14), each curve with a value in the set $\{-1, -0.9, -0.8, -0.7, 0.6, -0.5, -0.4, 0.3, -0.2, -0.1, 0, 0.1, 0.2, 0.3, 0.4, 0.5, 0.6, 0.7, 0.8, 0.9, 1\}$. We set t, ξ to be variables, and $\omega = -3/2$, $\xi_0 = 0$, $t \in [0, 4\pi]$, $\xi \in [-4\pi, 4\pi]$ in Figure 8 (a). Base on the figure, the solution is periodic on time t, and there are two parallel solutions with the same period and different amplitude at the peaks. When ξ ($\xi = \sum_{j=1}^{N} k_j x_j - ct$ can be interpreted as a space variable) is increasing, the solution decays, and the amplitude decreases and vanishes.

We set t, X to be variables, and $\omega = -3/2$, $\xi_0 = 0$, $t \in [0, 4\pi]$, $X \in [-4\pi, 4\pi]$ in Figure 8 (b). Base on the figure, (b) is a shift and rotation of (a). And similar to (a), the solution is periodic on time t. Moreover, close to the wave with the highest peaks, there are waves with the same period and smaller amplitude.

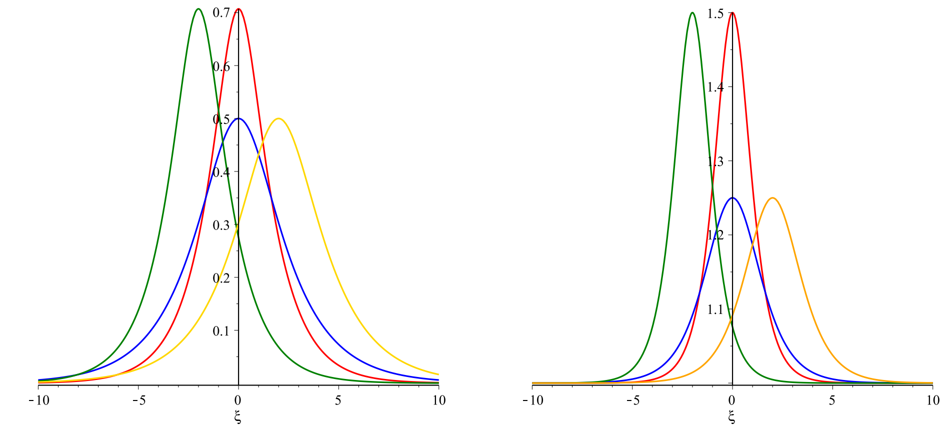

(a) $|u|$ (b) derivative of phase of u

Figure 5. (a) $|u|$ of the bright soliton (2.13)-(2.14): blue curve for $\omega = -3/2$, $\xi_0 = 0$; yellow curve for $\omega = -3/2$, $\xi_0 = -2$; red curve for $\omega = -5/4$, $\xi_0 = 0$; green curve for $\omega = -5/4$, $\xi_0 = 2$. (b) The phase profile of (a).

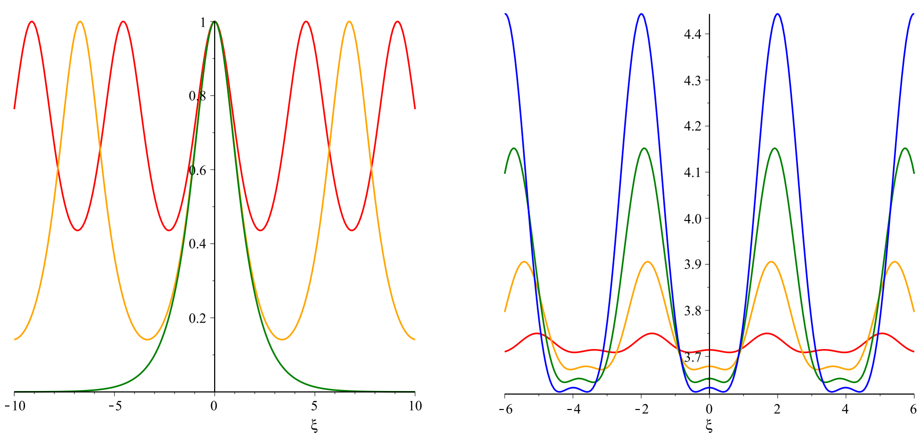

(a) $|u|$ (b) phase of u

Figure 6. (a) The solution $|u|$ of (3.5), $g(\xi) = \mathrm{dn}(\xi, R)$. $R = 9/10$, $R = 99/100$ and $R = 1$ are for the red, yellow and green curves respectively. (b) The total phase profile of $2-1/2\,k^{-2}+g^{-2}-1/2\,k^{-2}g^{-2}+g^2$ for the solution (3.5) where $g(\xi) = \mathrm{sn}(\xi, R))$ with $R = 1/2$(red), $R = 2/3$(yellow), $R = 3/4$(green) and $R = 4/5$(blue) respectively.

When X is increasing, the amplitude decreased and vanished. (v) For the solution (3.5), we set t and ξ to be variables, and plot contour curves of the 21 values $\{-1, -0.9, -0.8, -0.7, 0.6, -0.5, -0.4, 0.3, -0.2, -0.1, 0, 0.1, 0.2, 0.3, 0.4, 0.5, 0.6, 0.7, 0.8, 0.9, 1\}$. In Figure 9 (a), $g(\xi) = \mathrm{dn}(\xi, R)$, $R = 9/10$, $t \in [0, 4\pi]$ and $\xi \in [-2\pi, 2\pi]$. In Figure 9 (b), $g(\xi) = \mathrm{cn}(\xi, R)$, $R = \frac{3\sqrt{2}}{5}$, $t \in [0, 3\pi]$, $\xi \in [-2\pi, 2\pi]$. As we can see from the two figures, the solutions are periodic on time t, and some solutions are parallel. The solution is not decaying when ξ is increasing.

The solutions in Figure 8 and 9 are periodic as the corresponding solution has the factor $\mathrm{e}^{-i\omega t}$. And they have different decay rates because of the different phases

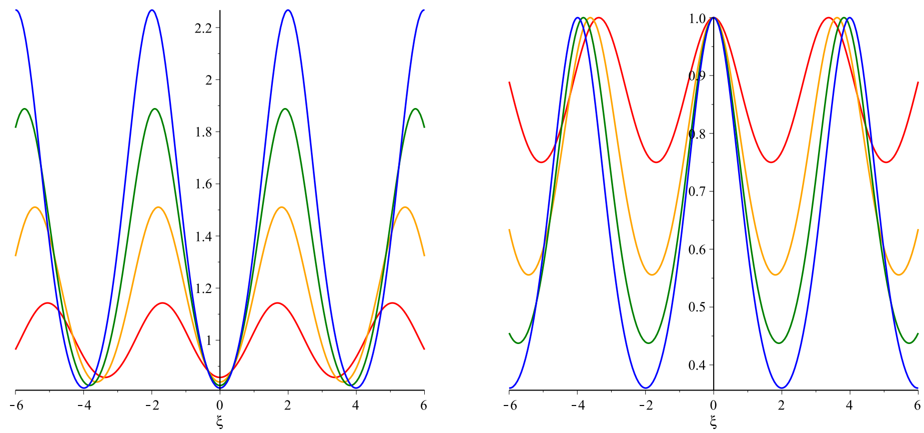

(a) kinematic (b) higher-order

Figure 7. Phase with the chirping reversal. $R = 1/2$(the red curve), $R = 2/3$(the yellow curve), $R = 3/4$(the green curve) and $R = 4/5$(the blue curve) respectively.

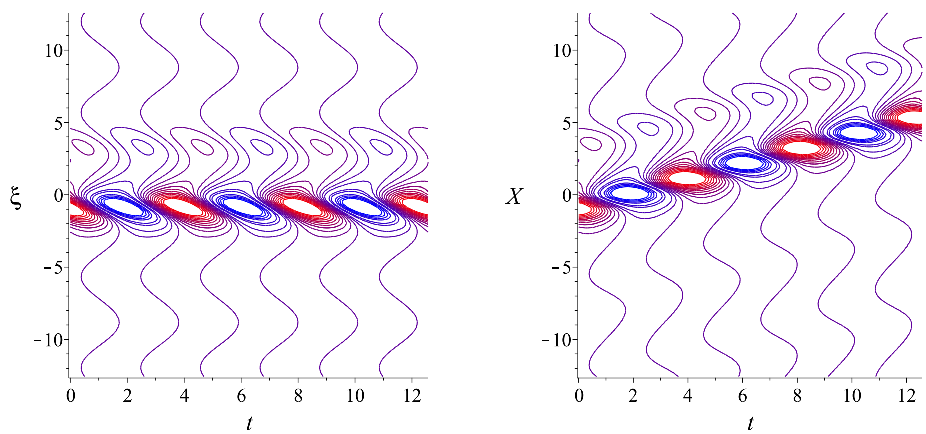

(a) solution (b) phase

Figure 8. (a) Contours of the real part of the bright soliton (2.13)-(2.14) depend on t and ξ (b) Contours of the real part of the bright soliton (2.13)-(2.14) depend on t and X ($\xi = X - \frac{t}{2}$).

in the corresponding solution. In (2.13)-(2.14), the phase factor is

$$\Theta_1 = 1 + g(\xi)^2,$$

which leads to the decay along ξ (or X) . The solution (3.5) has the phase factor

$$\Theta_2 = \frac{\left(1 + g(\xi)^2\right)\left(2\,dk^2 g(\xi)^2 + 2\,dk^2 - c\right)}{2\,g(\xi)^2 k^2},$$

and that g^2 and g^{-2} (this means there is kinematic chirping) canceled leads to no decay.

(vi) Choosing the same parameters as Figure 8 and Figure 9, we present the 3-dimensional real part of the solution (3.5) in Figure 10 and Figure 11. The real

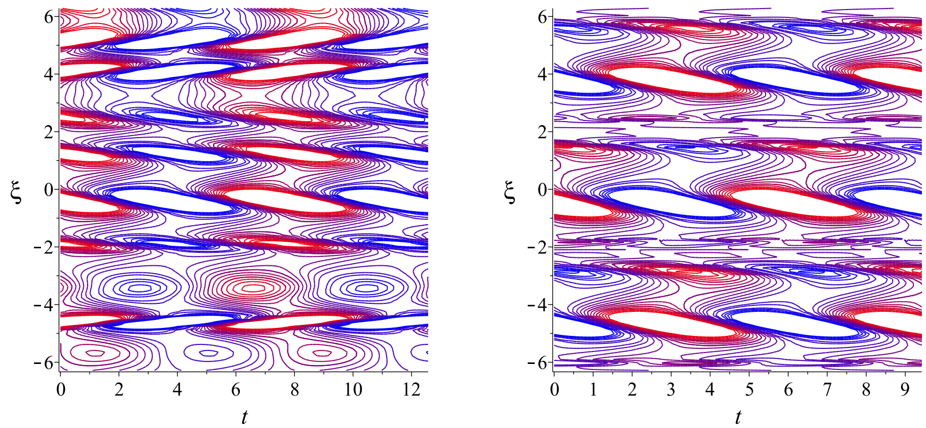

(a) solution (b) phase

Figure 9. (a) Contours of the real part of (3.5) with $g(\xi) = \mathrm{dn}(\xi, R)$ (b) Contours of the real part of (3.5) with $g(\xi) = \mathrm{cn}(\xi, R)$.

part of the soliton type solution (2.13) can be seen in Figure 10. In addition, the $\mathrm{dn}(\xi, R)$ type and the $\mathrm{cn}(\xi, R)$ type solution can be seen in Figure 11(a) and Figure 11(b) respectively. It is clear that the figures of these 3-dimensional solutions match their 2-dimensional contour map in Figure 8 and 9.

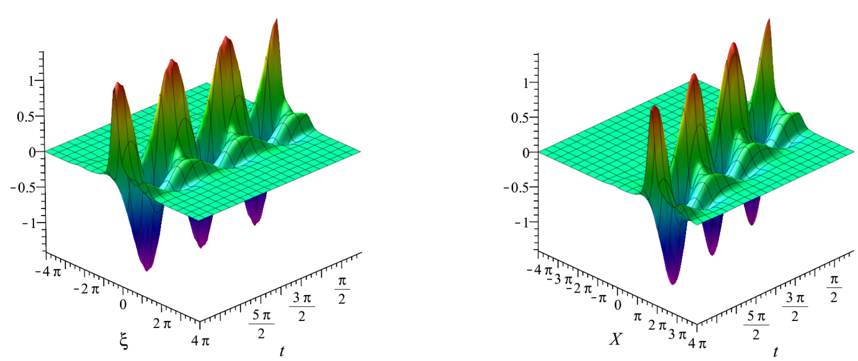

(a) solution 2.13 in ξ (b) solution 2.13 in x

Figure 10. (a) Figure of the solution 2.13 in terms of ξ. (b) Figure of the solution 2.13 in terms of x, where $\xi = x - \frac{t}{2}$. Note that this substitution shifts the peaks centered at $\xi = -\frac{\pi}{4}$ to different x.

(vii) Moreover, the $g(\xi)$ in (3.5) can be any of the following functions, $\mathrm{nc}(\xi, R)$(see (3.9)), $\mathrm{nd}(\xi, R)$ (see (3.10)) and $\frac{\mathrm{e}^{K\xi}}{2\,\mathrm{e}^{C_2 K} K} + \frac{\mathrm{e}^{C_2 K}\omega}{2\,\mathrm{e}^{K\xi} K}$ (see (3.11)). In Figure 12, we let $g(\xi) = \mathrm{nd}(\xi, R)$. Figure 12(a) shows the real part of the solution with $R = 3/5\sqrt{2}$, $t \in [0,\ 4\pi]$, $\xi \in [-2\pi,\ 2\pi]$. For a fixed ξ, the real part of the solution can be large (in fact, arbitrarily large), and this is determined by $\mathrm{nd}(\xi, R)$. In Figure 12(b), $|u|$ has the periodic singularities, In Figure 13, we let $g(\xi) = \mathrm{nd}(\xi, R)$. Figure 13(a)

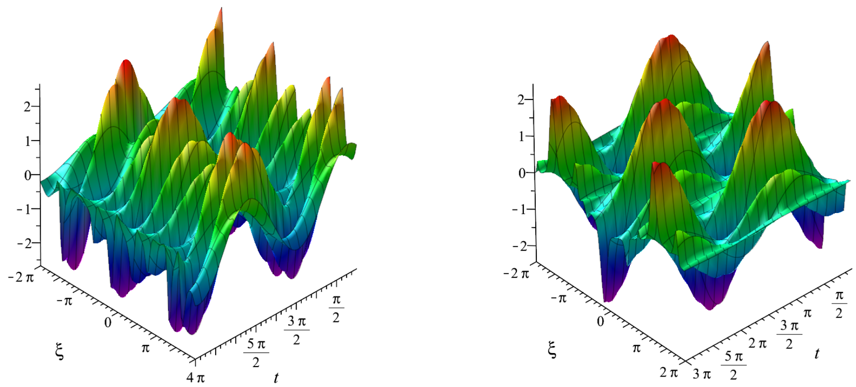

(a) solution 2.13 in ξ

(b) solution 2.13 in x

Figure 11. (a) The real part of (3.5) with $g(\xi) = \mathrm{dn}(\xi, R)$. (b) The real part of (3.5) with $g(\xi) = \mathrm{cn}(\xi, R)$.

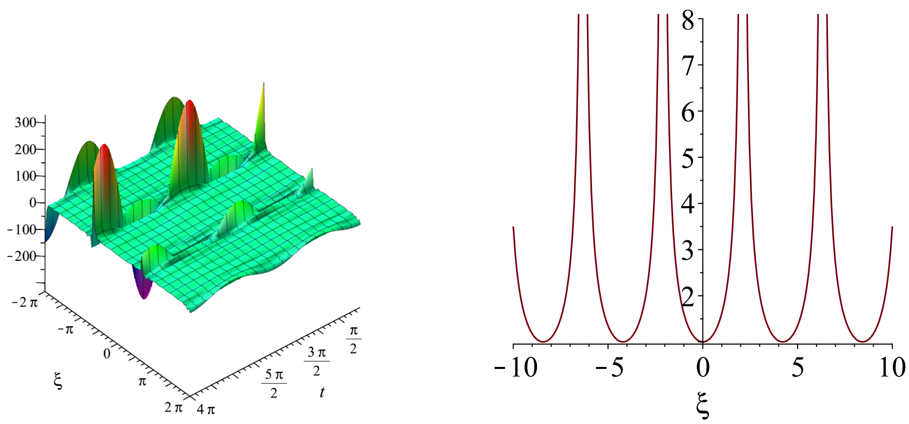

(a) solution 2.13 in ξ

(b) solution 2.13 in x

Figure 12. (a) The real part of (3.5) with $g(\xi) = \mathrm{nc}(\xi, R)$. (b) $|u|$ of the solution (3.5) with $g(\xi) = \mathrm{nc}(\xi, R)$

shows the real part of the solution with $R = 3/4$, $t \in [0,\ 6\pi]$, $\xi \in [-2\pi,\ 2\pi]$. The solution is periodic on time, t. On the ξ direction, the solution decays which is similar to the case $g(\xi) = \mathrm{cn}(\xi, R)$. Figure 13(b) shows that $|u|$ is a periodic and bounded function. In Figure 14, we let $g(\xi) = \frac{\mathrm{e}^{K\xi}}{2\,\mathrm{e}^{C_2 K} K} + \frac{\mathrm{e}^{C_2 K}\omega}{2\,\mathrm{e}^{K\xi} K}$. Figure 14(a) shows the real part of the solution with $k = 2$, $\omega = 1$, $C_2 = 1$, $c = 1$, $t \in [0,\ 4\pi]$, $\xi \in [-3/4\pi,\ 3/2\pi]$. The solution is periodic on the time t, and not periodic on ξ. Instead, when ξ is increasing, $|u|$ goes to infinity at an exponential rate, as we can see in Figure 14(b).

(viii) Figure 15 plots the solution of (2.16) and (3.6) with different $g(\xi)$. In Figure 15(a), the solution is given in (2.16), $g(\xi)$ is defined in (2.14). We set $\omega = -3/2$, $\xi_0 = 0$, $t = 5$ (the curves are similar even with different t), $\xi \in [-5\pi,\ 5\pi]$. In Figure

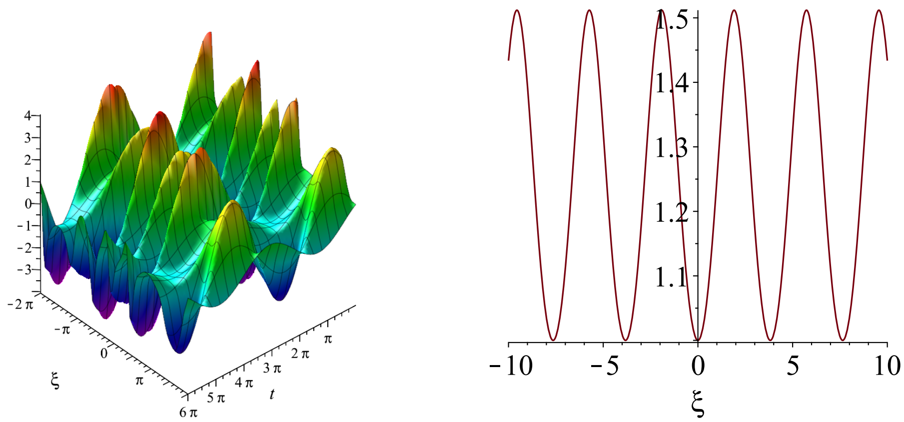

(a) solution 2.13 in ξ (b) solution 2.13 in x

Figure 13. (a) The real part of (3.5) with $g(\xi) = \mathrm{nd}(\xi, R)$. (b) $|u|$ of the solution (3.5) with $g(\xi) = \mathrm{nd}(\xi, R)$.

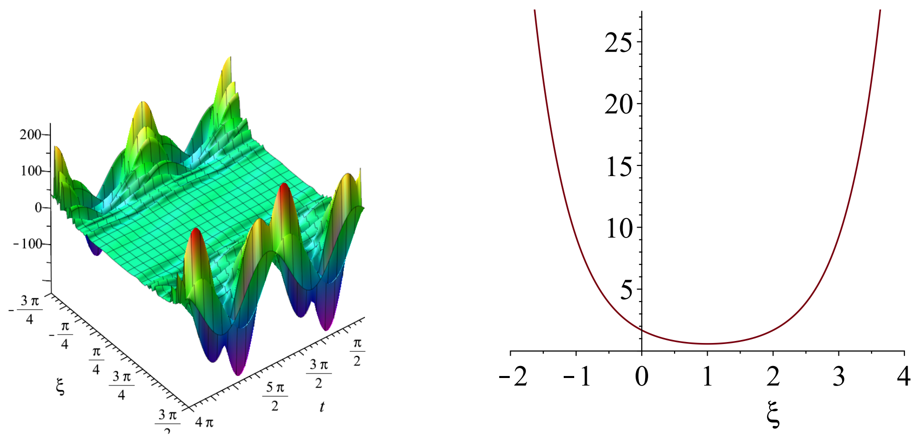

(a) solution 2.13 in ξ (b) solution 2.13 in x

Figure 14. (a) The real part of (3.5) with $g(\xi)$ in the form of (3.11. (b) $|u|$ of the solution (3.5) with $g(\xi)$ in the form of (3.11

15(a), the solution is plotted on various ξ. As we can see that when $|\xi|$ is increasing, the solution converges to the north pole of the sphere.

The solution (3.6) with $g(\xi)$ defined in (3.11) is shown in Figure 15(b). Here, we use the same parameters defined in the Figure 14, and let $t = 5$, $\xi \in [-5\pi,\ 5\pi]$. The solution is in the south hemisphere, and when $|\xi|$ is increasing, the solution converges to the south pole.

Note that whether the solution converges to the south or north pole is determined by S_3. In the solutions of (2.16) (or (3.6)) mentioned above, when $|\xi| \to +\infty$ (or $|\xi| \to C$), if

$$\frac{1 - |u|^2}{1 + |u|^2} \to 1,$$

then the solution converges to the north pole, and if

$$\frac{1-|u|^2}{1+|u|^2} \to -1,$$

then the solution converges to the south pole.

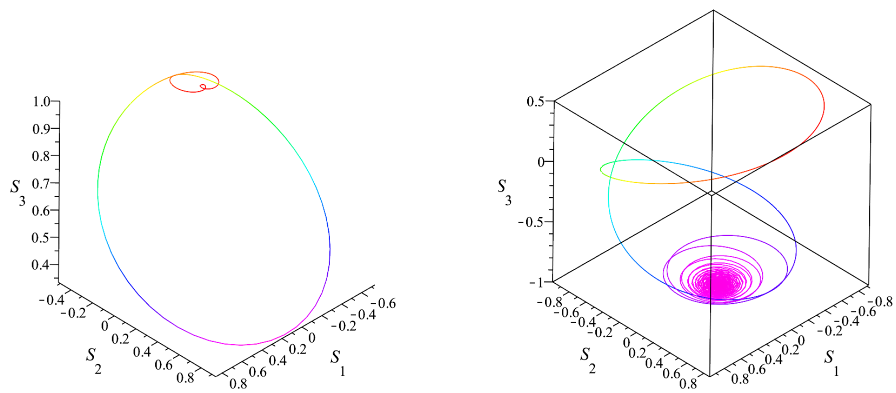

(a) solution (2.16) in ξ

(b) solution (2.16) in X

Figure 15. (a) Solution (2.16) with $g(\xi)$ in the form of (2.14). (b) Solution (3.6) with $g(\xi)$ in the form of (3.11).

(ix) Figure 16 shows the four types of solution of Theorem 3.1 as defined in (2.16). The parameters are selected in accordance with those used in Figures 11-13, the difference is that we set $t = 5$ in Figure 16(a)(d) (as other values t results similar curves), and $\xi \in [-5\pi,\ 5\pi]$. Figure 16(a) is the case $g(\xi) = \mathrm{dn}(\xi, R)$. In this case, the solution is no longer converging monotonous to either the north pole or the south pole. When $|\xi|$ is increasing, the solution spirals up and down on the sphere. Similarly, Figure 16(d), where $g(\xi) = \mathrm{nd}(\xi, R)$, is similar to Figure 16(a) except that the solution is bounded on the south hemisphere.

The solution for $g(\xi) = \mathrm{cn}(\xi, R)$ is shown in Figure 16(b), and it spirals up and down in the north hemisphere, it overlaps with north pole and equator. And the solution for $g(\xi) = \mathrm{nc}(\xi, R)$ in Figure 16(c) is similar to (b) except that the solutions are in the south hemisphere.

6. Comparison of the different solutions

In this section, we compare our solution with some other solutions of the equivalent equations of the LL equation. The ILLE in (1.4) can also be reduced to another complex NLSE without the derivative term. If we define the curvature κ (it can be regarded as a gradient flow) and the torsion τ to be

$$\kappa = (S_{x_1} \cdot S_{x_1})^{\frac{1}{2}}\,, \quad \text{and} \quad \tau = \frac{S \cdot (S_{x_1} \times S_{x_1 x_1})}{\kappa^2}, \tag{6.1}$$

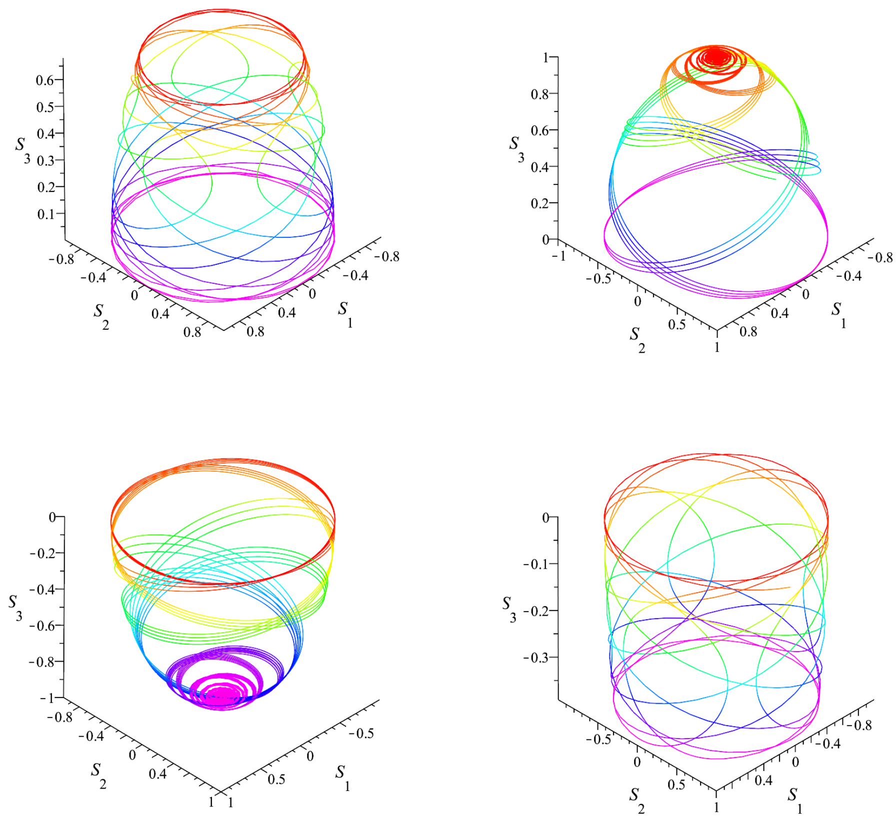

Figure 16. (a) Solution 3.6 with with $g(\xi)$ in the form of (3.7. (b) Solution 3.6 with with $g(\xi)$ in the form of (3.8. (c) Solution 3.6 with with $g(\xi)$ in the form of (3.9. (d) Solution 3.6 with with $g(\xi)$ in the form of (3.10.

then by applying the Hasimoto transformation in [27],

$$u = \kappa \exp\left(\mathrm{i}\int_{-\infty}^{x_1} \tau\left(t, x'\right) \mathrm{d}x'\right).$$

the equation (1.4) can be converted to the following NLSE,

$$iu_t + u_{x_1 x_1} + \frac{1}{2} u \left|u\right|^2 = 0. \tag{6.2}$$

To solve (6.2) one can assume a solution

$$u(t,\, x_1) = \varphi(t,\, x_1) \mathrm{e}^{i\hat{\theta}(t,\, x_1)} \tag{6.3}$$

where $\varphi(t,\, x_1) = \varphi(\xi)$ and $\hat{\theta}(t,\, x_1) = \theta(\xi) + \Omega t$, and these are real functions with $\xi = x_1 - vt$, where v and Ω are arbitrary parameters, and Ω is the propagation velocity of the non-linear excitation. In [1], the authors use the ansatz (6.3) to construct the solution of (6.2) and obtain the following,

$$\varphi(\xi) = (\gamma/8\delta)^{\frac{1}{2}} \operatorname{sech}((\gamma/4\delta)\xi) \tag{6.4}$$

and

$$\theta(\xi) = \frac{V\xi}{2} + \tan^{-1}\left\{\left(\frac{\beta^2}{1-\beta^2}\right)^{\frac{1}{2}} \tanh\left(\beta\gamma^{\frac{1}{2}}.\xi\right)\right\}.$$

where γ, δ, β and V are some constant coefficients.

As we can see from expression (6.4) this solitary wave (6.3) has the property that as we increase γ the amplitude of the envelope function φ becomes larger. In this way, the solution (6.3) indicates that the classical envelope soliton represents the magnon-bound state which pointed out by Schneider and Stoll [32].

Comparing solution (6.3) and solution (1.5), we can see that the solution has a similar structure of traveling wave solution. But we also see that the solution we present in this paper contains some more subtype solutions. These sub cases include soliton type solutions, periodic solutions (such as $\operatorname{dn}(\xi, R)$, $\operatorname{cn}(\xi, R)$, etc.) and double exponential solutions. Specifically, the envelope soliton (6.3) and the associated phenomena represent merely the classical limit of magnon bound states and their effect on properties of interest. According to (1.5), the state of the solution is not only this magnon state, but also contains more ground states that is not time dependent.

It is worth noting that, the solution of (1.4) can be transformed into the solution of (6.2) easily. However, to obtain the solution of (1.4) from the solution of (6.2), solving an additional nonlinear partial differential equation is needed. If we use (1.3) to study (1.4), the transformation between the solutions of these two equations is very easy.

Indeed, the ILLE is equivalent to Schrödinger flow under a complex transformation. If S satisfies (1.4), then we define u as the stereographic projection of S by

$$u = \frac{S_1 + iS_2}{1 - S_3}. \tag{6.5}$$

It is easy to verify that u is the solution of (1.3). Conversely, let S be

$$S = \left(\frac{\pm 2\mathrm{Re}u}{1+|u|^2}, \frac{\pm 2\mathrm{Im}u}{1+|u|^2}, \frac{1-|u|^2}{1+|u|^2}\right), \tag{6.6}$$

where $\mathrm{Re}u$ and $\mathrm{Im}u$ is the real and imaginary parts of complex function u respectively. Then (1.4) reduces to (1.3). Furthermore, there exits some connections between $|\nabla u|$ and $|\nabla S|$. We can estimate $|\nabla S|$ using $|\nabla u|$. With S being

$$S_1 = \frac{2\mathrm{Re}u}{1+|u|^2}, \quad S_2 = \frac{2\mathrm{Im}u}{1+|u|^2}, \quad \text{and} \quad S_3 = \frac{1-|u|^2}{1+|u|^2},$$

we compute the gradient

$$\nabla S_1 = \frac{2\mathrm{Re}(\nabla u)}{1+|u|^2} - \frac{4\mathrm{Re}u\mathrm{Re}(\bar{u}\nabla u)}{(1+|u|^2)^2},$$

$$\nabla S_2 = \frac{2\mathrm{Im}(\nabla u)}{1+|u|^2} - \frac{4\mathrm{Im}u\mathrm{Re}(\bar{u}\nabla u)}{(1+|u|^2)^2},$$

and

$$\nabla S_3 = -\frac{4\mathrm{Re}\,(\bar{u}\nabla u)}{\left(1+|u|^2\right)^2}.$$

As

$$\frac{2}{1+a^2} \le 2 \quad \text{and} \quad \frac{4a}{\left(1+a^2\right)^2} \le 1 \quad (a \ge 0),$$

we have that

$$\begin{aligned}
\sqrt{|\nabla S_1|^2 + |\nabla S_2|^2} &= |\nabla S_1 + i\nabla S_2| \\
&\le |\nabla u| \left(\frac{2}{1+|u|^2} + \left| \frac{2u\,(\bar{u}\nabla u + u\nabla \bar{u})}{\left(1+|u|^2\right)^2} \right| \right) \\
&\le 3|\nabla u|, \\
|\nabla S_3| \le \left| \frac{2\,(\bar{u}\nabla u + u\nabla \bar{u})}{\left(1+|u|^2\right)^2} \right| &\le 2|\nabla u|.
\end{aligned}$$

Therefore,

$$|\nabla S| = \sqrt{|\nabla S_1|^2 + |\nabla S_2|^2 + |\nabla S_3|^2} \le \sqrt{13}|\nabla u|. \tag{6.7}$$

In addition, for the solution $u\,(t,\,\xi) = \mathrm{e}^{-i\omega\,t}\mathrm{e}^{if(\xi)}g\,(\xi)$, we have

$$\frac{\mathrm{d}}{\mathrm{d}\xi}u\,(t,\,\xi) = \mathrm{e}^{i(-\omega\,t+f(\xi))}\left(i\left(\frac{\mathrm{d}}{\mathrm{d}\xi}f\,(\xi)\right)g\,(\xi) + \frac{\mathrm{d}}{\mathrm{d}\xi}g\,(\xi)\right). \tag{6.8}$$

Combine (6.7) and (6.8), we have that

$$|\nabla S| \le C\left(\left|\left(\frac{\mathrm{d}}{\mathrm{d}\xi}f\,(\xi)\right)g\,(\xi)\right| + \left|\frac{\mathrm{d}}{\mathrm{d}\xi}g\,(\xi)\right|\right),$$

further combine the three definitions of $g(\xi)$ and $f(\xi)$ in Table (4), we obtain that $|\nabla S| < +\infty$. This property can also be verified in Figure 15 and 16, the gradients of all the solutions are infinity.

In other words, $|\nabla u|$ can be estimated by $|\nabla S|$. As

$$u = \frac{S_1 + iS_2}{1+S_3},$$

with the direct computation,

$$|\nabla u| \le |\left(1+S_3\right)^{-1}|\left(|\nabla S_1| + |\nabla S_2|\right) + |\nabla S_3||\left(1+S_3\right)^{-2}|\left(|S_1| + |S_2|\right).$$

Assume that $\inf S_3 \ge -1+\delta$, $\delta \in (0,\ 2]$, with $|S| = 1$, we have that

$$|\nabla u| \le \delta^{-2}\left(|\nabla S_1| + |\nabla S_2| + |\nabla S_3|\right).$$

Therefore, if δ is fixed and $|\nabla S|$ is finite, then $|\nabla u|$ is also finite.

As we can see in Figure 16 (a) and (d), δ and $|\nabla S|$ are finite, within the range of the parameters we defined, $|\nabla u|$ is not singular.

In [43], the authors constructed several types of exact solutions of (1.4) which include the standing wave solution represented in polar coordinates (r, χ) as follows

$$S(t,\,r) = \left(\sin\left(\phi\,(r)\right)\cos\left(m\chi + \omega\,t + \zeta\right),\ \sin\left(\phi\,(r)\right)\sin\left(m\chi + \omega\,t + \zeta\right),\ \cos\left(\phi\,(r)\right)\right),$$

and the equivalent solution of (1.3) as

$$u(t,\, r, \chi) = \frac{\sin\left(\phi\left(r\right)\right)}{1+\cos\left(\phi\left(r\right)\right)}\mathrm{e}^{i(m\chi+\omega\, t+\zeta)} \tag{6.9}$$

where m is a vortex degree, ω is the angular velocity (frequency) and ζ is the initial phase.

Similarly, the authors also established the solution for ILLE as

$$S(t,\, x_1,\, x_2) = \left(\cos(\omega t+\zeta)\sin\Theta,\ \sin(\omega t+\zeta)\sin\Theta,\ \cos\Theta\right),$$

where $\Theta = \theta\left(x_1,\, x_2\right)$. Then the equivalent solution of (1.3) is

$$u(t,\, x_1,\, x_2) = \frac{\sin\Theta}{1+\cos\Theta}\mathrm{e}^{i(\omega t+\zeta)} \tag{6.10}$$

where $\Theta = \pm 2\arctan(f(\xi_1)g(\xi_2))$, $\xi_1 = ax_1+b$, $\xi_2 = cx_2+d$. In fact, the two dimensional case $u(t,\, x_1,\, x_2)$ can be extended to the three dimensional solution (see [43])

$$u(t,\, x_1,\, x_2,\, x_3) = \frac{\sin\left(\theta\left(x_1,\, x_2,\, x_3\right)\right)}{1+\cos\left(\theta\left(x_1,\, x_2,\, x_3\right)\right)}\mathrm{e}^{i(\omega t+\zeta)}, \tag{6.11}$$

where $\theta\left(x_1,\, x_2,\, x_3\right) = \arctan(f(\xi_1)g(\xi_2)q(\xi_3))$, $\xi_1 = ax_1+b$, $\xi_2 = cx_2+d$, $\xi_3 = kx_3+m$.

Specifically, the above solutions (6.9) and (6.10) (or (6.11)) are vorticity type solution and traveling wave type solution respectively. These two kinds of solutions are very different from the solutions (1.5) we construct in this paper. Firstly, the solution of vorticity type is in polar coordinates, with cylindrical symmetry variable r. Hence, r can not be transformed into traveling wave variable, and this solution does not belong to traveling wave type solution. Secondly, the traveling wave solution (6.10) (or (6.11)) is a variable separated traveling wave solution, in which there are two (ξ_1 and ξ_2) or three traveling wave variables (ξ_1, ξ_2 and ξ_3). This indicates that in addition to the multiple traveling wave variables solutions, there also exists many single travelling wave variable solutions.

For convenience, we listed various solutions of the equivalent equation of (1.4) in Table 5.

7. Conclusions

In summary, Schrödinger flow (at the same time for ILLE) is studied and some solutions are given in this paper. These solutions include domain wall arrays and bright solitons. We also exclude several special types of solutions, such as the kink profile solution, singular solution, triangular periodic solution, singular triangular periodic solution, fronts, and dark solitons. As we know, various modern methods were proposed to obtain the exact solutions of the systems arising in mathematical physics. However, in order to better understand the dynamic characteristics of this equation, it needs to be solved more accurately. Therefore, we use the homogeneous balance principle and general Jacobi elliptic-function method to obtain the exact solutions. These explicit traveling wave solutions (in the form of $\mathrm{e}^{-i\omega\, t}\mathrm{e}^{if(\xi)}g\left(\xi\right)$) of the Schrödinger flow are based on the different ODEs given. These are powerful methods in solving the PDE.

Table 5. Solutions of the equivalent equation of (1.4).

Equations I-V	u
$iu_t + u_{x_1x_1} + \frac{1}{2}u\,\lvert u\rvert^2 = 0$	$u(t,\, x) = \varphi(\xi)\mathrm{e}^{i\theta(\xi)}\mathrm{e}^{i\Omega t}$, $\xi = x_1 - vt$
$iu_t = -\triangle_{(r,\chi)}u + \frac{2\bar{u}}{1+\lvert u\rvert^2}(\nabla_{(r,\chi)}u)^2$	$u(t,\, r, \chi) = \frac{\sin(\phi(r))}{1+\cos(\phi(r))}\mathrm{e}^{i(m\chi+\omega\, t+\zeta)}$
$iu_t = -\triangle_{(x_1,x_2)}u + \frac{2\bar{u}}{1+\lvert u\rvert^2}(\nabla_{(x_1,x_2)}u)^2$	$u(t,\, x_1,\, x_2) = \frac{\sin(\theta(x_1,\, x_2))}{1+\cos(\theta(x_1,\, x_2))}\mathrm{e}^{i(\omega t+\zeta)}$, $\theta(x_1, x_2) = \pm 2\arctan(f(\xi_1)g(\xi_2))$, $\xi_1 = ax_1 + b$, $\xi_2 = cx_2 + d$
$iu_t = -\triangle_{(x_1,x_2,x_3)}u + \frac{2\bar{u}}{1+\lvert u\rvert^2}(\nabla_{(x_1,x_2,x_3)}u)^2$	$u(t,\, x_1,\, x_2,\, x_3) = \frac{\sin(\theta(x_1,\, x_2,\, x_3))}{1+\cos(\theta(x_1,\, x_2,\, x_3))}\mathrm{e}^{i(\omega t+\zeta)}$, $\theta\,(x_1,\, x_2,\, x_3) = \arctan(f(\xi_1)g(\xi_2)q(\xi_3))$, $\xi_1 = ax_1 + b$, $\xi_2 = cx_2 + d$, $\xi_3 = kx_3 + m$
$iu_t = -\triangle_{(x_1,\ldots,x_n)}u + \frac{2\bar{u}}{1+\lvert u\rvert^2}(\nabla_{(x_1,\ldots,x_n)}u)^2$	$u(t,\, x_1,\, \ldots,\, x_N) = \mathrm{e}^{-i\omega\, t}\mathrm{e}^{if(\xi)}g\,(\xi)$, $\xi = \sum\limits_{j=1}^{N} k_jx_j - ct$

It is interesting that the traveling solutions of the Schrödinger flow change with respect to the different ODEs. These equations (some of these ODEs can be solved exactly) can not be converted to the Hamiltonian systems. Hence, we analyze the phase and singular point of the equivalent equations derived from these ODEs. The phase portraits change with respect to the changes of the parameters. Moreover, the coordinates of the possible center point of the limit cycle are computed.

The exact solutions we obtained are all periodic in time t while the solutions are not periodic in ξ due to the phase Θ_1 (or Θ_2). Because Θ_2 has both g^2 and g^{-2} (meaning the kinematic chirping term exists), the Jacobi elliptic function type solution does not decay to 0 as $\xi \to \infty$. However, the bright soliton will decay to 0 due to the single factor g^2 in the phase Θ_1.

8. Acknowledgements

The first author is supported by National Outstanding Youth Science Fund Project of National Natural Science Foundation of China (No. 11601092), Special Innovation Projects of Universities in Guangdong Province (No. 2018KTSCX161), Special Projects in Key Areas of Guangdong Province (No. ZDZX1088) and Fund for Science and Technology of Guangzhou (No. 202102080428).

References

[1] L. G. de Azevedo, M. A. de Moura, C. Cordeiro and B. Zeks, *Solitary waves in a 1D isotropic Heisenberg ferromagnet*, Journal of Physics C: Solid State Physics, 1982, 15, 7391–7396.

[2] I. Bejenaru, A. D. Ionescu and C. E Kenig, *Global existence and uniqueness of Schrödinger maps in dimensions $d \geq 4$*, Adv. Math., 2007, 215, 263–291.

[3] I. Bejenaru, A. D. Ionescu, C. E. Kenig and D. Tataru, *Global Schrödinger maps in dimensions $d \geq 2$: Small data in the critical Sobolev spaces*, Annals of Mathematics, 2011, 173(3), 1443–1506.

[4] G. Berkolaiko and P. Kuchment, *Introduction to quantum graphs*, Mathematical Surveys and Monographs. Providence, RI: American Mathematical Society, 2013.

[5] A. Biswas, *Chirp-free bright optical solitons and conservation laws for complex Ginzburg-Landau equation with three nonlinear forms*, Optik, 174, 207–215, 2018.

[6] P. A. Clarkson and J. A. Tuszynski, *Exact solutions of the multidimensional derivative nonlinear Schrödinger equation for many-body systems of criticality*, Journal of Physics A: Mathematical and General, 1990, 23(19), 4269–4288.

[7] C. Dai, Y. Wang and C. Yan, *Chirped and chirp-free self-similar cnoidal and solitary wave solutions of the cubic-quintic nonlinear Schrödinger equation with distributed coefficients*, Optics Communications, 2010, 283(7), 1489–1494.

[8] L. G. de Azevedo, M. A. de Moura, C. Cordeiro and B. Zeks, *Solitary waves in a 1d isotropic Heisenberg ferromagnet*, Journal of Physics C: Solid State Physics, 1982, 15(36), 7391–7396.

[9] Q. Ding, *Explicit blow-up solutions to the Schr¨odinger maps from R^2 to the hyperbolic 2-space H^2*, Journal of Mathematical Physics, 2009, 50(10), 103507.

[10] S. Ding and C. Wang, *Finite time singularity of the landau-lifshitz-gillbert equation*, International Mathematics Research Notices, 2007.

[11] J. M. Dudley, G. Genty and B. J. Eggleton, *Harnessing and control of optical rogue waves in supercontinuum generation*, Optics Express, 2008, 16(6), 3644.

[12] B. Guo and G. Yang, *Some exact nontrivial global solutions with values in unit sphere for two-dimensional landau–lifshitz equations*, Journal of Mathematical Physics, 2001, 42(11), 5223–5227.

[13] D. Huang, D. Li and H. Zhang, *Explicit and exact travelling wave solutions for the generalized derivative Schrödinger equation*, Chaos, Solitons and Fractals, 2007, 31, 586–593.

[14] V. G. Ivancevic, *Adaptive-wave alternative for the black-scholes option pricing model*, 2009.

[15] B. Jalali, P. Koonath, C. Ropers and D. R. Solli, *Optical rogue waves*, Nature, 2007, 450, 1054–1057.

[16] V. V. Konotop, Y. V. Bludov and N. Akhmediev, *Matter rogue waves*, Phys. Rev. A, 2009, 80, 033610.

[17] C. Kosaka, K. Nakamura, S. Murugesh and M. Lakshmanan, *Equatorial and related nonequilibrium states in magnetization dynamics of ferromagnets: Generalization of suhl's spin-wave instabilities*, Physica D, 2005, 203, 233–248.

[18] M. Lakshmanan, *The fascinating world of landau-lifshitz-gilbert equation: An overview*, Philos. Trans. A Math. Phys. Eng., 2011, 369, 1280–1300.

[19] L. D. Landau and E. M. Lifshitz, *On the theory of the dispersion of magnetic permeability in ferromagnetic bodies*, Reproduced in Collected Papers of L. D. Landau, Pergamon, New York, 2011, 101–114.

[20] F. Merle, P. Raphaël and I. Radnianski, *Blowup dynamics for smooth data equivariant solutions to the critical Schrödinger map problem*, Invent. Math., 2013, 193(2), 249–365.

[21] E. Mjølhus, *Nonlinear Alfvén waves and the DNLS equation: Oblique aspects*, Phys. Scr., 1989, 40, 227–237.

[22] K. Ohkuma, Y. H. Ichikawa and Y. Abe, *Soliton propagation along optical fibers*, Optics Letters, 1987, 12(7), 516.

[23] M. Onorato, D. Proment, G. Clauss and M. Klein, *Rogue waves: from nonlinear Schrödinger breather solutions to sea-keeping test*, PLoS One, 2013.

[24] R. Parmentier, *The New Superconducting Electronics*, Springer, chapter Solitons and Long Josephson Junctions, 1993.

[25] G. Perelman, *Blow up dynamics for equivariant critical Schrödinger maps*, Comm. Math. Phys., 2014, 330(1), 69–105.

[26] V. M. Pérez-García, H. Michinel, J. I. Cirac, M. Lewenstein and P. Zoller, *Dynamics of bose-einstein condensates: Variational solutions of the gross-pitaevskii equations*, Phys. Rev. A, 1997, 56, 1424–1432.

[27] K. Porsezian, K. Tamizhmani and M. Lakshmanan, *Geometrical equivalence of a deformed Heisenberg spin equation and the generalized nonlinear Schrödinger equation*, Physics Letters A, 1987, 124(3), 159–160.

[28] R. Radhakrishnan and M. Lakshmanan, *Bright and dark soliton solutions to coupled nonlinear Schrödinger equations*, Journal of Physics A: Mathematical and General, 1995, 28(9), 2683–2692.

[29] H. Rezazadeh, *New solitons solutions of the complex Ginzburg-Landau equation with Kerr law nonlinearity*, Optik, 2018, 167, 218–227.

[30] J. Rogel-Salazar, *The gross-pitaevskii equation and bose-einstein condensates*, European Journal of Physics, 2013, 34(2), 247–257.

[31] P. A. Ruprecht, M. J. Holland, K. Burnett and M. Edwards, *Time-dependent solution of the nonlinear Schrödinger equation for Bose-condensed trapped neutral atoms*, Phys. Rev. A, 1995, 51, 4704–4711.

[32] T. Schneider and E. Stoll, *Excitation spectrum of ferromagnetic Heisenberg chains*, Journal of Applied Physics, 1982, 53, 1850.

[33] L. Stenflo and M. Marklund, *Rogue waves in the atmosphere*, Journal of Plasma Physics, 2010, 76(3–4), 293–295.

[34] C. Sulem and P. L. Sulem, *Focusing nonlinear schrödinger equation and wave-packet collapse*, Nonlinear Analysis: Theory, Methods & Applications, Proceedings of the Second World Congress of Nonlinear Analysts, 1997, 30(2), 833–844.

[35] H. Susanto, N. Karjanto, Zulkarnain, T. Nusantara and T. Widjanarko, *Soliton and breather splitting on stargraphs from tricrystal josephson junctions*, Symmetry, 2019, 11(2).

[36] J. Tjon and J. Wright, *Solitons in the continuous Heisenberg spin chain*, Physical Review B, 1977, 15(7), 3470–3476.

[37] E. van Groesen, Andonowati and N. Karjanto, *Displaced phase-amplitude variables for waves on finite background*, Physics Letters A, 2006, 354(4), 312–319.

[38] M. Wang, J. Zhang and X. Li, *Solitary wave solutions of a generalized derivative nonlinear Schrödinger equation*, Commun. Theor. Phys., 2008, 50, 39–42.

[39] B. Xia, Z. Qiao and J. Li, *An integrable system with peakon, complex peakon, weak kink, and kink-peakon interactional solutions*, Communications in Nonlinear Science and Numerical Simulation, 2018, 63, 292–306.

[40] Z. Yan, *Financial rogue waves*, Communications in Theoretical Physics, 2010, 54(5), 947–949.

[41] V. E. Zaltharov and A. B. Shabat, *Exact theory of two-dimensional self-focusing and one-dimensional self-modulation of waves in nonlinear media*, Journal of Experimental and Theoretical Physics, 1972, 34, 62–69.

[42] D. Zhao, Y. Zhang, W. Lou and H. Luo, *AKNS hierarchy, Darboux transformation and conservation laws of the 1D nonautonomous nonlinear Schrödinger equations*, J. Math. Phys., 2011, 52(4), 043502–16.

[43] P. Zhong, S. Wang and S. Chen, *Some periodic and blow-up solutions for landau–lifshitz equation*, Modern Physics Letters A, 2011, 26(32), 2437–2452.

[44] P. Zhong, S. Wang and M. Zeng, *Some exact blowup solutions to multidimensioanal schrödinger map equation on hyperbolic spaec and cone*, Modern Physics Letters A, 2013, 28(10), 1350043.

[45] P. Zhong, R. Yang and G. Yang, *Exact periodic and blow up solutions for 2D Ginzburg-Landau equation*, Physics Letters A, 2008, 373(1), 19–22.